CONTRACTOR REPORT

SAND84-8181
UC-62d
Unlimited Release

10 MWe Solar Thermal Central Receiver Pilot Plant Mode 1 (Test 1110) Test Report

McDonnell Douglas Astronautics Company
Huntington Beach, California

Prepared by Sandia National Laboratories, Albuquerque, New Mexico 87185 and Livermore, California 94550 for the United States Department of Energy under Contract DE-AC04-76DP00789.

Printed October 1984

Issued by Sandia National Laboratories, operated for the United States Department of Energy by Sandia Corporation.

Printed in the United States of America
Available from
National Technical Information Service
5285 Port Royal Road
Springfield, VA 22161

NTIS price codes
Printed copy: A04
Microfiche copy: A01

10 MWe SOLAR THERMAL
CENTRAL RECEIVER PILOT PLANT

MODE 1 (TEST 1110) TEST REPORT

ABSTRACT

Solar One is the world's largest solar thermal central receiver electric power plant. It is currently in the midst of a two-year Experimental Test and Evaluation phase which began in August 1982.

The plant is designed to operate in 8 basic operating modes (including shutdown) which are intended to demonstrate and fully exercise the energy collection, energy storage, and power generation features of a central receiver system. During Mode 1 operation, which is the subject of this report, all of the collected solar energy is converted into superheated steam in the receiver with the steam then flowing directly to the turbine for electrical power production. Neither the charging nor discharging features of the thermal storage system are involved in this operation.

This report contains baseline plant design information pertinent to Mode 1 operation and presents the results of the Mode 1 test activities. The Test Results section of the report includes information regarding steady state plant performance at both design and off design conditions, plant startup and shutdown transitions, and plant trips.

CONTENTS

ILLUSTRATIONS

TABLES

MODE 1 TEST REPORT SUMMARY

Solar One is the largest solar thermal central receiver plant in the world. Since April, 1982, the plant has been in the process of starting up major systems and performing preliminary operational evaluation. The testing and evaluation will continue into 1984 and beginning in August, 1984 the plant will be turned over to Southern California Edison for the prime purpose of energy production.

The purpose of this report is to document plant operation and testing in the mode where all solar power is absorbed by the receiver and flows directly to the turbine in the form of high pressure, high temperature steam (Mode 1).

Test results reported here show that plant level performance is optimal at steam pressures and temperatures below the design level of 1450 psi and 960^{o}F. This conclusion is based upon four factors;

1. the turbine performance is relatively insensitive to steam temperature;

2. improvements in turbine expansion efficiency and reduced turbine control valve losses are experienced at higher steam flows and lower operating steam pressure;

3. receiver thermal losses are lower at a lower operating steam temperature, and

4. lower parasitic power load is associated with a lower steam pressure.

Plant operation at less than design temperature and pressure has posed no particular operating problems even though an increase in system steam flow results for a given absorbed receiver power level. This is due to the fact that insolation levels from December, 1982 through June, 1983 are 15 to 20% below the 1976 design baseline values. In addition, the turbine is slightly oversized (rated for 12.5 MW) and thus is capable of accepting mass flows above design levels.

During the testing reported here, it has been demonstrated that the turbine-generator could be repeatably synchronized within two to 2.5 hours of sunrise and operated until forty-five minutes before sunset. A midday start required one to 1.5 hours. Trip sequences involving the turbine and receiver demonstrated that the trip logic and controlled shutdown sequences were properly executed to protect plant equipment and maintain safe operation.

1.0 Introduction

Solar One is the world's largest solar-thermal central receiver power plant. It is designed to produce 10 MWe net power for 4 hours on a design winter day and for 7.8 hours on a design summer day. The plant is also designed to generate 7 MWe net power for up to 4 hours from stored thermal energy.

The principal elements of the system are shown schematically in Figure 1.1. They include the collector system which consists of 1818 heliostats surrounding the central tower, a water-steam single-pass external receiver, a thermal storage system which stores heat in a single tank filled with oil and rock, separating the hot and cold regions by a thermocline temperature boundary, and a standard steam Rankine electrical power generation cycle. Detailed information regarding the design and operation of each of these plant systems is contained in Reference 1.

With these systems, it is possible to operate the plant in any of 8 basic operating modes. The energy flow paths for each of the 8 operating modes are depicted in Figure 1.2.

The purpose of this report is to document plant operation and testing in Mode 1 (Turbine Direct). In this mode, all of the redirected power which is absorbed by the receiver flows directly to the turbine in the form of high temperature, high pressure steam. While operating in this mode, neither the thermal storage charging nor extraction systems are in service.

The principal components and flow paths associated with the feedwater and steam systems which are active during Mode 1 operation are shown in Figure 1.3. The feedwater circuit starts at the condenser and flows through 4 stages of feedwater heating enroute to the receiver. Steam which is produced by the single pass to superheat receiver flows through the main steam downcomer and directly to the turbine. Other possible steam flow paths shown in the figure involve auxiliary steam service (through PV1003), steam dump system operation (through PV1001 and FV1006), and through 4 bootleg (low point) drain valves which flow to the condenser. Also shown in the figure are the relative locations of the principal process instrumentation used in monitoring and evaluating Mode 1 operation.

2.0 Test Goals and Objectives

The goals and objectives of this Mode 1 test program were to gather test data in four areas of plant operation for subsequent analysis and comparison to design requirements. These are steady state operation, startup and transition testing, trips involving the turbine and receiver, and off design operations involving alternate steam temperature and pressure conditions to support special sensitivity studies.

2.1 Steady State Mode 1 Plant Requirements and Test Objectives

The basic Mode 1 design requirements were that the plant shall be capable of producing 10 MWe net for 7.8 hours on a "design summer day" and for 4 hours

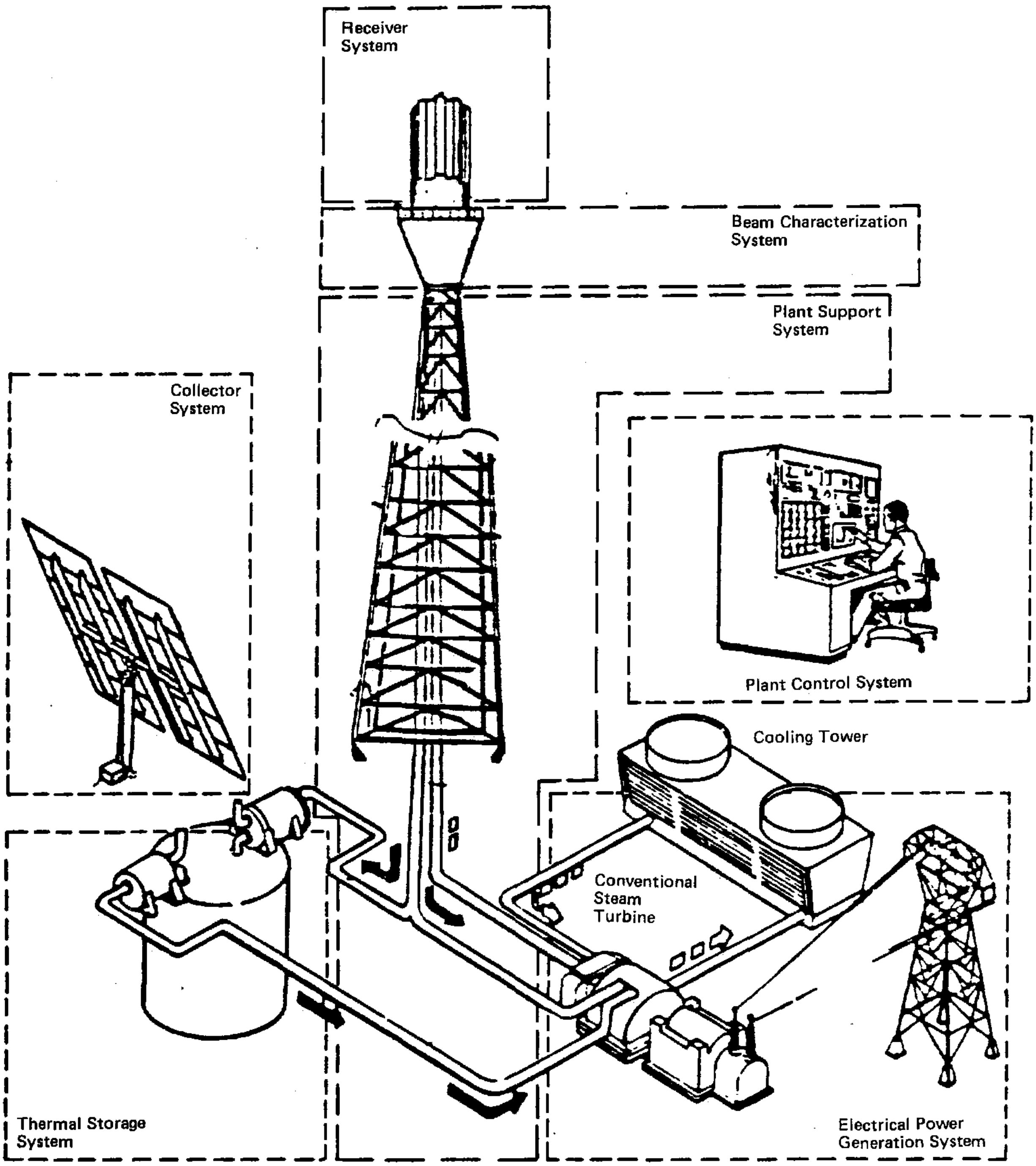

Figure 1.1. Solar One System Schematic

on a "design winter day". Implicit in the design summer and winter days are assumptions regarding the direct insolation, heliostat reflectivity, and heliostat availability. The insolation profiles used to design the plant are shown in Figure 2.1. The corresponding assumption for field average heliostat specular reflectivity is 0.89* with a corresponding heliostat availability of 100%*.

---

*Design assumptions as specified by the DOE project office during design.

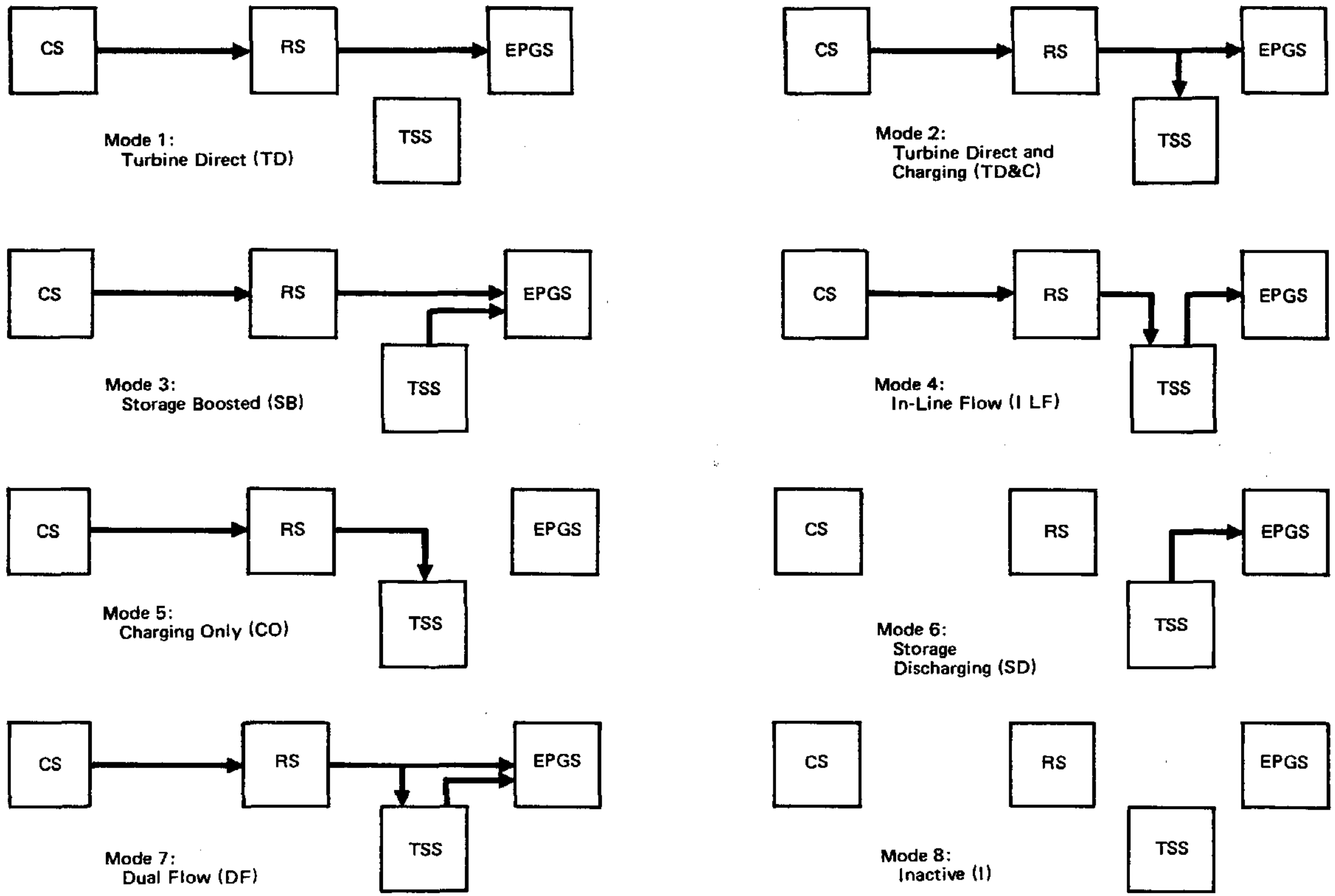

CS — Collector System
RS — Receiver System
TSS — Thermal Storage System
EPGS — Electrical Power Generation System

Figure 1.2. Solar One Plant Operating Modes

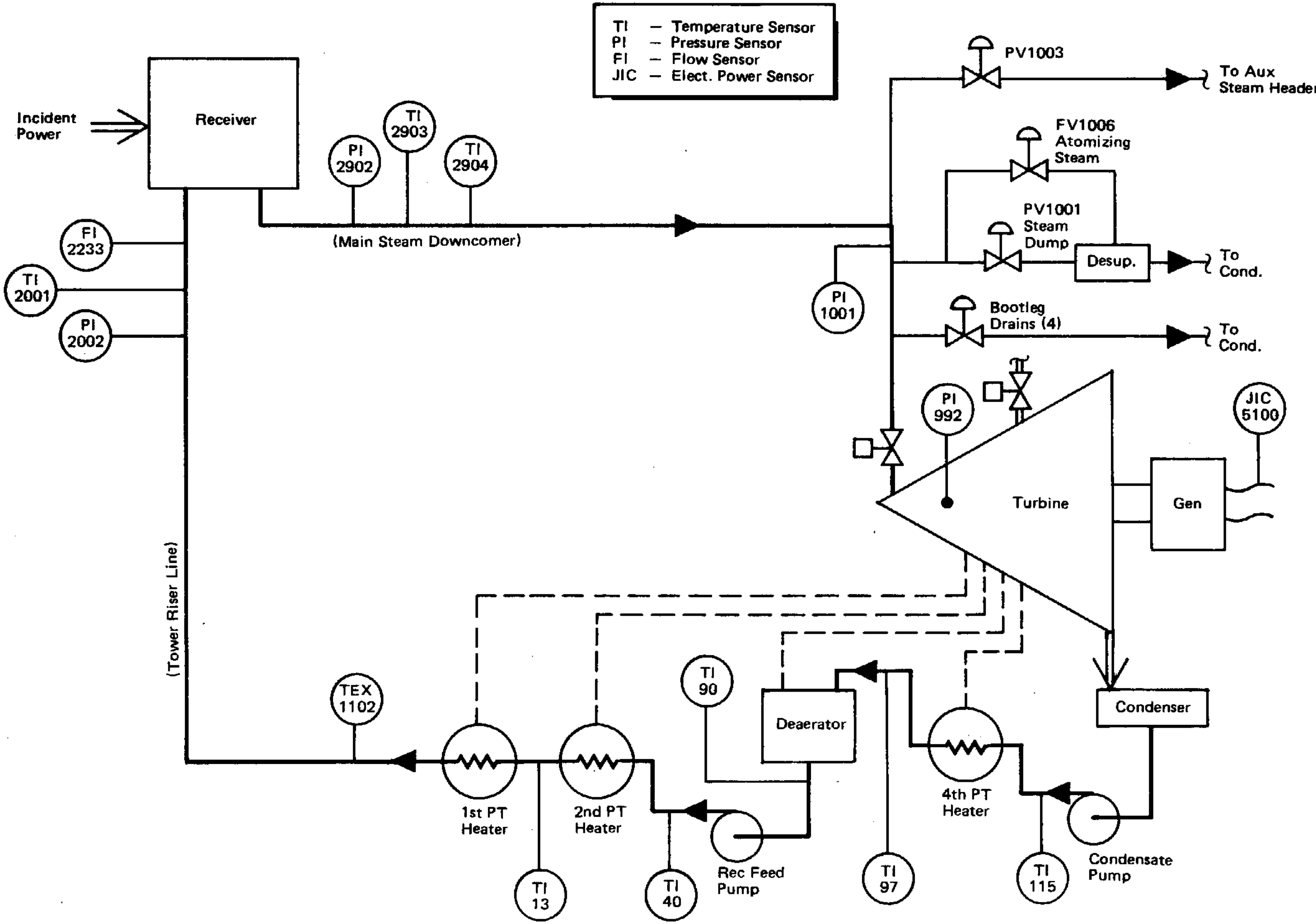

Figure 1.3. Mode 1 Flow Path and Principal Instrumentation

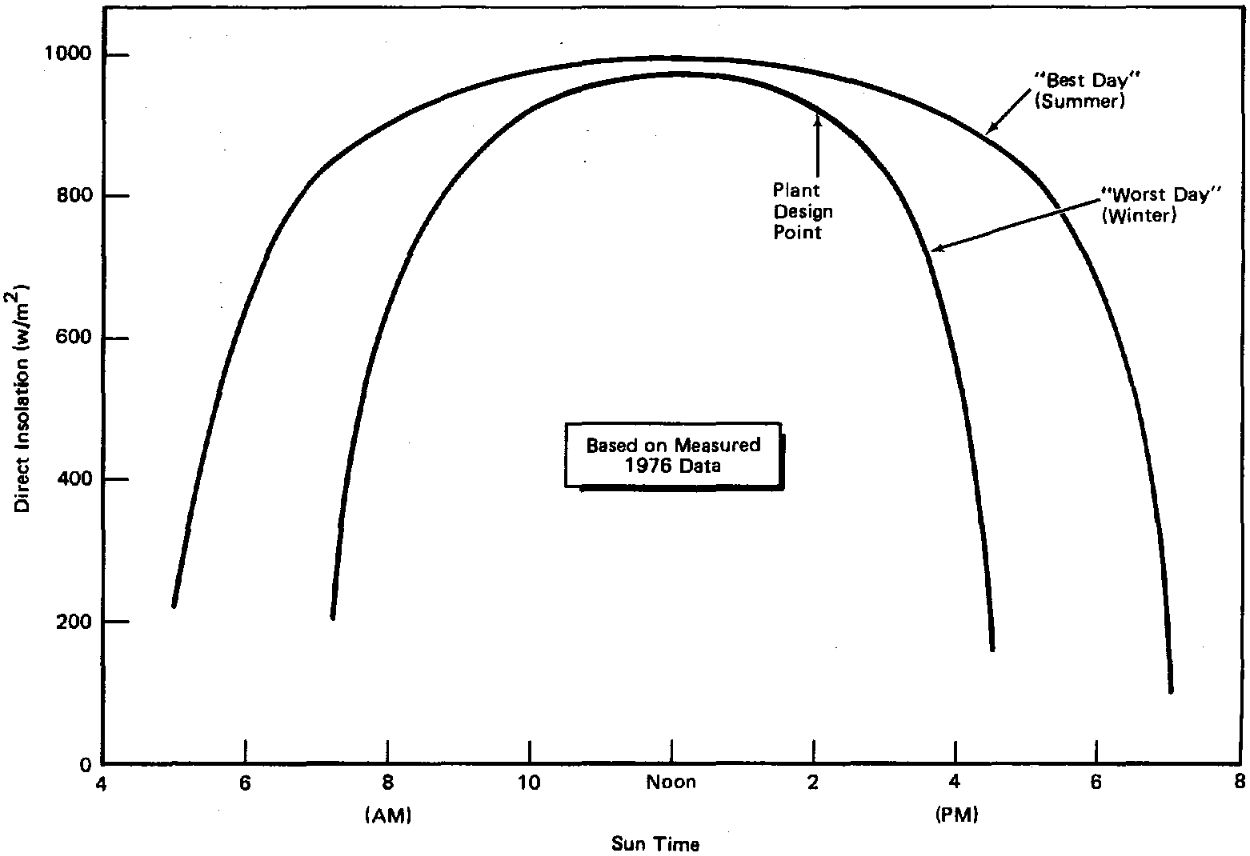

Figure 2.1. "Design Day" Insolation Models

Prior to initiating detailed plant design, the summer and winter operating time periods were screened to identify the limiting instant in time (minimum power point) for plant sizing purposes. Consideration was given to the simultaneous affects of insolation, collector field "cosine" loss, and heliostat blocking and shadowing losses. The resulting analysis indicated that the minimum power point would occur at winter 2 PM (sun time) and thus, the plant was sized for a winter 2 PM design point.

One of the steady state test objectives involved demonstrating the degree to which the power levels and durations stated above could be satisfied recognizing that the actual values of insolation, heliostat reflectivity, and heliostat availability may deviate significantly from the design values. The other principal steady state test objective involved gathering full and part power performance data to compare to predicted plant performance estimates and to determine the minimum threshold power for Mode 1 operation.

2.2 <u>Plant Startup and Transition Test Objectives</u>

The requirements for plant startup and transitions are that the plant shall be capable of being started up and transitioned into Mode 1 operation. The plant shall also be capable of being shutdown from Mode 1 operation. In addition, the plant shall be capable of transitioning between low and high power levels as a routine part of Mode 1 operation.

Although no times for these startup, shutdown, and transition operations were established as part of the plant design requirements, the implicit goal is to accomplish these operations in a timely fashion. Testing in these areas involved developing baseline timeline data and identifying system, component, and operator constraints. From this information, limiting hardware and operational related issues were identified for future investigation.

2.3 Trips

The stated requirement involving trips is that the plant shall be capable of transitioning to a safe condition (or shutting down if appropriate) if an anomalous (trip) condition exists. Types of trips appropriate for investigation during Mode 1 operation are turbine trips and receiver trips. The principal test objectives are to verify that the proper trip sequence is executed and that the plant transitions to a safe condition.

From an actual test planning standpoint, no dedicated trip tests were specified. Instead, sufficient data were gathered during naturally occurring trips that occurred during routine operation as a result of either process upsets or instrumentation malfunctions.

2.4 Sensitivity Studies

The goal of the sensitivity studies was to determine the preferred operating conditions (steam temperature and pressure) which maximize Mode 1 performance and to determine the magnitude of the performance penalty associated with operation away from the peak performance condition. These types of tests were not included in the original test planning but were included when intuitive insight seemed to indicate that improvements in plant performance could be realized by operating at something other than design steam conditions. Implicit in these studies is the influence of steam temperature and pressure on the combined receiver-turbine cycle efficiency.

3.0 Plant Design Summary

Before discussing plant test results for Mode 1 operation, it is appropriate to review basic performance predictions that were developed as part of the initial plant sizing and overall design activities. With this information, it is possible to make direct comparisons to actual operating data and to identify areas of discrepancy or uncertainty against which further investigations and analysis can be made.

A summary of the overall plant design point (Winter 2 p.m.) performance predictions along with the peak power (Summer noon) predictions are contained in Figure 3.1 (based on information contained in Reference 2). The efficiency Waterfall" format starts at the left side with the thermal power incident on the heliostats if all heliostats were oriented normal to the incoming sun light. The waterfall attempts to account for all of the performance factors that would be experienced as the thermal power flows through the collector and receiver systems and is ultimately converted to electricity in the turbine cycle. The specific loss mechanism for each of the waterfall steps is listed along with the corresponding efficiency or thermal loss factor.

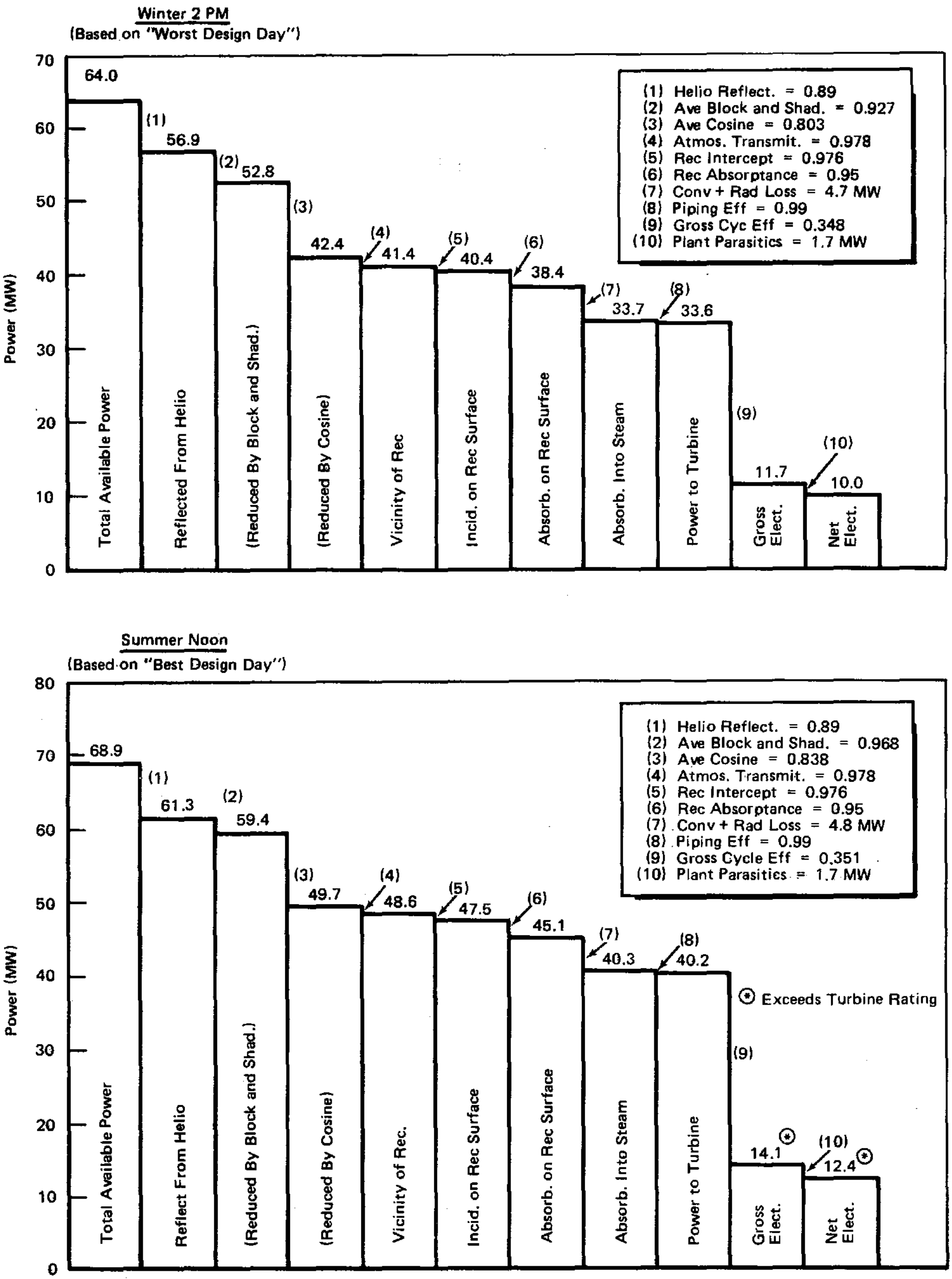

Figure 3.1. Solar One Mode 1 Design "Waterfall Efficiency" Chart

The heliostat reflectivity value of 0.89 which appears in both of the waterfall charts was a specified assumption (by the Department of Energy) to be used in all plant sizing and design calculations. This allows for a slight degradation from the field average clean reflectivity of 0.906 which represents an area weighted average for the mixture of low and high iron (glass) heliostats used in the Solar One field.

The indicated values for heliostat blocking and shadowing and collector field cosine in both cases represent area weighted average values for the entire collector field. They were calculated based on "as built" heliostat locations and the instantaneous orientation of adjacent heliostats assuming all heliostats were tracking the receiver. Tabulations of field average blocking and shadowing and field average cosine factors appropriate to various times of day and days of the year were developed in Reference 3 and are contained in Tables 3.1 and 3.2. Due to daily and seasonal symmetry, the 7 x 7 array of numbers contained in each table actually represents 13 instants of time on 12 days spaced throughout the year.

Table 3.1. Collector Field Average Blocking and Shadowing Performance Factors (Prepared by the University of Houston November 1981)

		(Solar Noon)						(10^0 Sun Elev)
	Hour =	0.	1.05	2.09	3.14	4.18	5.23	6.28
Day =	93	0.9682	0.9670	0.9682	0.9726	0.9705	0.9190	0.7341
	Hour =	0.	1.02	2.04	3.06	4.07	5.09	6.11
Day =	124	0.9674	0.9667	0.9682	0.9723	0.9698	0.9187	0.7288
	Hour =	0.	0.95	1.90	2.85	3.81	4.76	5.71
Day =	155	0.9664	0.9668	0.9688	0.9714	0.9665	0.9123	0.7245
	Hour =	0.	0.86	1.72	2.59	3.45	4.31	5.17
Day =	186	0.9680	0.9684	0.9695	0.9694	0.9569	0.8951	0.7113
	Hour =	0.	0.77	1.53	2.30	3.06	3.83	4.60
Day =	216	0.9683	0.9683	0.9675	0.9619	0.9376	0.8690	0.7001
	Hour =	0.	0.68	1.36	2.04	2.71	3.39	4.07
Day =	246	0.9631	0.9616	0.9558	0.9418	0.9083	0.8375	0.6953
	Hour =	0.	0.64	1.28	1.92	2.56	3.20	3.85
Day =	276	0.9564	0.9541	0.9460	0.9288	0.8925	0.8240	0.6883

Legend: "Hour" - Hours from Solar Noon (appropriate to morning or afternoon)
Day 93 - June 21 (summer solstice)
124 - May 21 or July 22
155 - April 20 or Aug 22
186 - March 20 or Sept 22 (equinox)
216 - Feb 18 or Oct 22
246 - Jan 19 or Nov 21
276 - Dec 21 (winter solstice)

Table 3.2. Collector Field Average Cosine Performance Factors (Prepared by the University of Houston November, 1981)

		(Solar Noon)						(10° Sun Elev)
	Hour =	0.	1.05	2.09	3.14	4.18	5.23	6.28
Day =	93	0.8376	0.8315	0.8134	0.7842	0.7451	0.6978	0.6451
	Hour =	0.	1.02	2.04	3.06	4.07	5.09	6.11
Day =	124	0.8406	0.8346	0.8172	0.7888	0.7506	0.7043	0.6524
	Hour =	0.	0.95	1.90	2.85	3.81	4.76	5.71
Day =	155	0.8455	0.8401	0.8242	0.7983	0.7632	0.7203	0.6714
	Hour =	0.	0.86	1.72	2.59	3.45	4.31	5.17
Day =	186	0.8463	0.8418	0.8284	0.8065	0.7767	0.7399	0.6974
	Hour =	0.	0.77	1.53	2.30	3.06	3.83	4.60
Day =	216	0.8409	0.8374	0.8269	0.8098	0.7863	0.7570	0.7229
	Hour =	0.	0.68	1.36	2.04	2.71	3.39	4.07
Day =	246	0.8327	0.8300	0.8221	0.8090	0.7910	0.7685	0.7420
	Hour =	0.	0.64	1.28	1.92	2.56	3.20	3.85
Day =	276	0.8288	0.8264	0.8195	0.8080	0.7922	0.7724	0.7489

Legend: "Hours" - Hours from Solar Noon (appropriate to morning or afternoon)
Day 93 - June 21 (summer solstice)
124 - May 21 or July 22
155 - April 20 or Aug 22
186 - March 20 or Sept 22 (equinox)
216 - Feb 18 or Oct 22
246 - Jan 19 or Nov 21
276 - Dec 21 (winter solstice)

The value for atmospheric transmittance (0.978) was analytically determined based on assumptions for water vapor and aerosols consistent with a dry desert environment. No attempt was made during the plant design activities to include values as a function of time of day or season.

The receiver interception factor (0.976) represents a field average value. It was calculated by the existing University of Houston collector field performance computer codes based on a set of heliosat assumptions regarding tracking accuracy, surface waviness, and structural rigidity which were consistent with the heliostat procurement specification. No attempt was made as part of the baseline plant sizing task to include the impacts of variations in wind speed, ambient temperature, or differing aim strategies on the interception factor. It was also assumed that all heliostats were perfectly aligned to the proper receiver aim point following their initial installation.

The receiver absorption value of 0.95 was based on the "new" absorptivity characteristics of pyromark. No additional allowance was included for possible degradation of the coating as a result of receiver exposure to concentrated sunlight or natural weathering affects.

The convection and radiation loss values reflect seasonal differences in ambient temperature and wind speed which, based on existing correlations involving natural and forced convection, directly influence overall convection loss. The higher summer time losses result from the higher average summer wind speed (14.5 mph vs 8.5 mph for winter day average operating periods). The corresponding summer and winter day average temperatures used for convective loss calculations were 87°F and 55°F respectively. The piping loss value (1% of maximum power) is based on heat loss and change in thermodynamic state point conditions experienced by the steam as it passes through the downcomer and to the turbine.

The gross cycle efficiency assumptions which occur in the turbine generator cycle are based on published GE performance data based on the turbine guaranteed performance in conjunction with a four feedwater heater cycle. The difference in efficiencies shown in Figure 3.1 reflect the effect of higher power level (steam flow) associated with summer noon operation. The detailed variations in power level as a function of throttle steam flow and the resulting gross heat rate are shown in Figure 3.2 (taken from Ref. 4). The plant parasitic power estimate is based on the simultaneous power demand for all electrical equipment that would normally be operational during Mode 1.

Detailed data involving actual state point conditions at various points around the water/steam portion of the system, as presented in Reference 5, are shown in Figures 3.3A and B for the 10 MWe design point condition (winter 2 p.m.). Explicit in these data are turbine inlet conditions of 950°F and 1450 psi and a condenser pressure of 2.5 in Hg. The impact of varying the condenser pressure in terms of incremental change in electrical output is shown in Figure 3.4 (taken from Ref. 4). The figure shows the significant advantage to be realized in running the turbine at a minimum exhaust pressure.

4.0 Test Approach and Critical Measurements

The approach to Mode 1 testing involved developing a sufficient operational data base so that both steady state and transition operations could be thoroughly analyzed. This included plant operations at both design and off design operating conditions.

In general, a significant portion of this data base was developed as part of routine power production operations carried out on weekends and during holiday periods as well as during dedicated power production tests. Additional Mode 1 operations which were required to develop data at specific test conditions were accomplished during dedicated periods of the (weekday) test program. Data involving trips during Mode 1 operation were gathered during naturally occurring trips that occurred as part of routine plant operations. No dedicated trip tests were conducted.

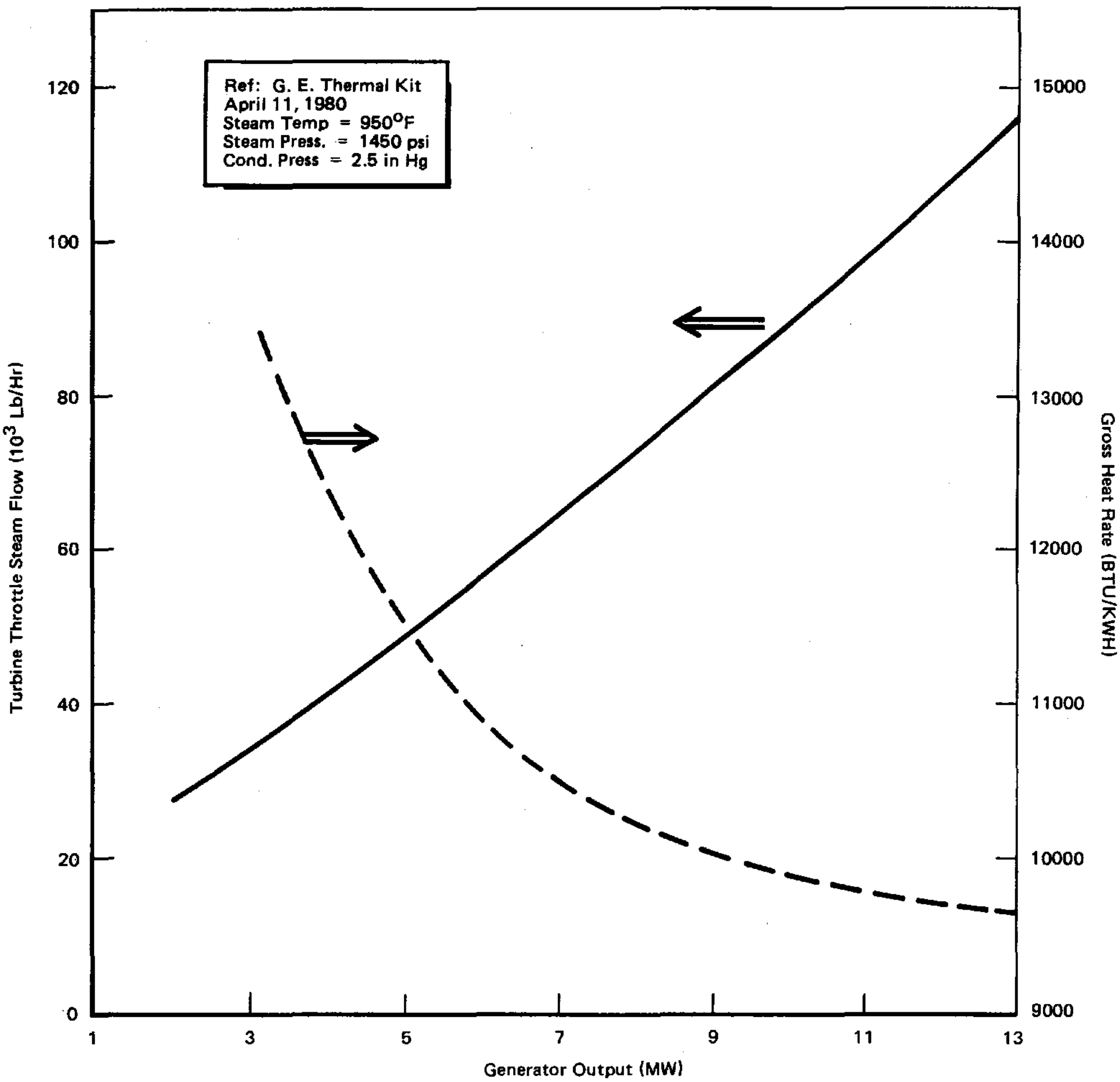

Figure 3.2. Baseline Turbine Cycle Performance Characteristics

Table 4.1 presents the Mode 1 operating data base that served as the basis for this report. It covers the time period from mid December 1982 to mid July 1983. These days were selected since they contained substantial periods of steady state Mode 1 operation at a variety of operating conditions as well as data pertaining to transitions and trips.

The plant evaluation associated with the water/steam cycle during Mode 1 operation was based on the principal process measurements listed in Table 4.2. Also contained in this table is the instrument range for each measurement.

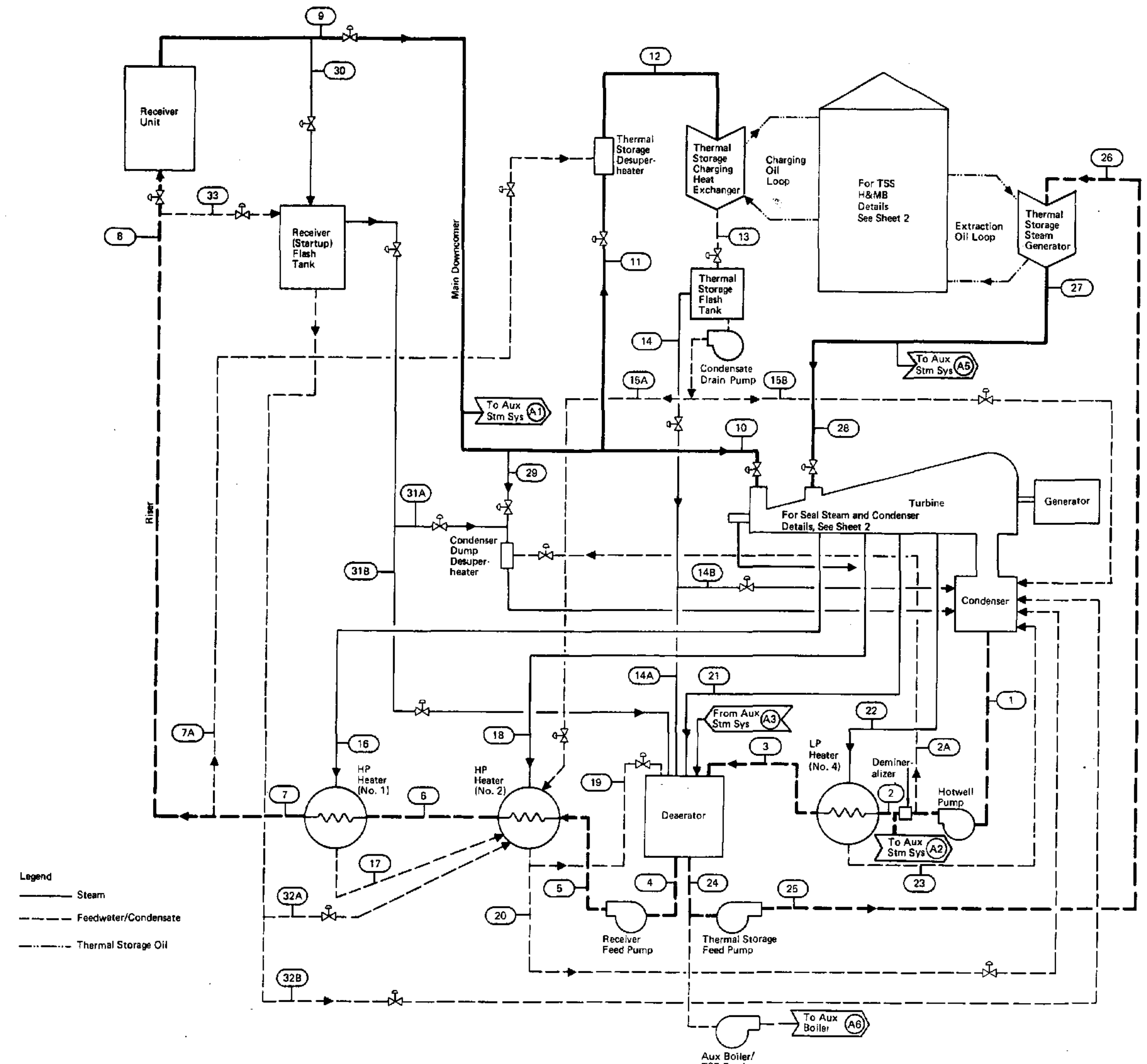

Summary	
Operating Mode	1
Total Turbine Generator Gross Output	11.72 MWe
Plant Auxiliary Power	1.69 MWe
Plant Net Electrical Output	10.03 MWe
Receiver Absorbed Power	33.616 MWt
Cycle Heat Rate	9785.1 BTU/KWH
Condenser Duty	74.741 MBTU/HR

Comments:

- Mode 1 – 10 MWe Design

Location Number	Flowrate (lb/hr)	Enthalpy (Btu/lb)	Temperature (°F)	Pressure (psia)
1	86621.1	76.7	108.7	1.228
2	86621.1	77.1	108.8	140.0
2A	0			
3	86621.1	162.6	194.3	137.2
4	105150.0	231.1	262.3	36.84
5	105150.0	240.7	267.5	1899.0
6	105150.0	306.3	331.9	1894.8
7	105150.0	374.6	397.3	1890.6
7A	0			
8	105150.0	374.6	397.3	1777.0
9	105150.0	1466.4	960.0	1535.0
10	105150.0	1461.0	950.0	1466.0
11				
12				
13				
14				
14A				
14B				
15A				
15B				
16	7067.8	1328.7	622.2	251.62
17	7067.8	312.3	340.8	251.62
18	5410.8	1433.2	808.2	111.96
19	12478.6	245.7	276.4	111.96
20				
21	6050.2	1182.4	291.2	36.84
22	7223.7	1110.2	202.2	11.22
23	7223.7	85.3	117.2	11.22
24				
25				
26				
27				
28				
29				
30				
31A				
31B				
32A				
32B				
33				

DEPARTMENT OF ENERGY
SAN FRANCISCO OPERATIONS OFFICE

SOLAR TEN MEGAWATT PROJECT OFFICE
9550 FLAIR DRIVE, SUITE 210
EL MONTE, CALIFORNIA 91731

10 MWe SOLAR PILOT PLANT - DAGGETT, CALIFORNIA

SOLAR FACILITIES DESIGN INTEGRATOR

McDONNELL DOUGLAS · Stearns-Roger · Rockwell International Rocketdyne Division

STEARNS-ROGER
ROCKETDYNE
MDAC
SFDI

TITLE
HEAT AND MASS BALANCE
MODE 1-2

DRAWING NO 40O1003133901

SHEET NO 1 OF 2

REV 1

REVISIONS · REFERENCE DRAWINGS · PRINT RECORD

3

Figure 3.3A. Heat and Mass Balance Mode 1 (10 MW Design Point)

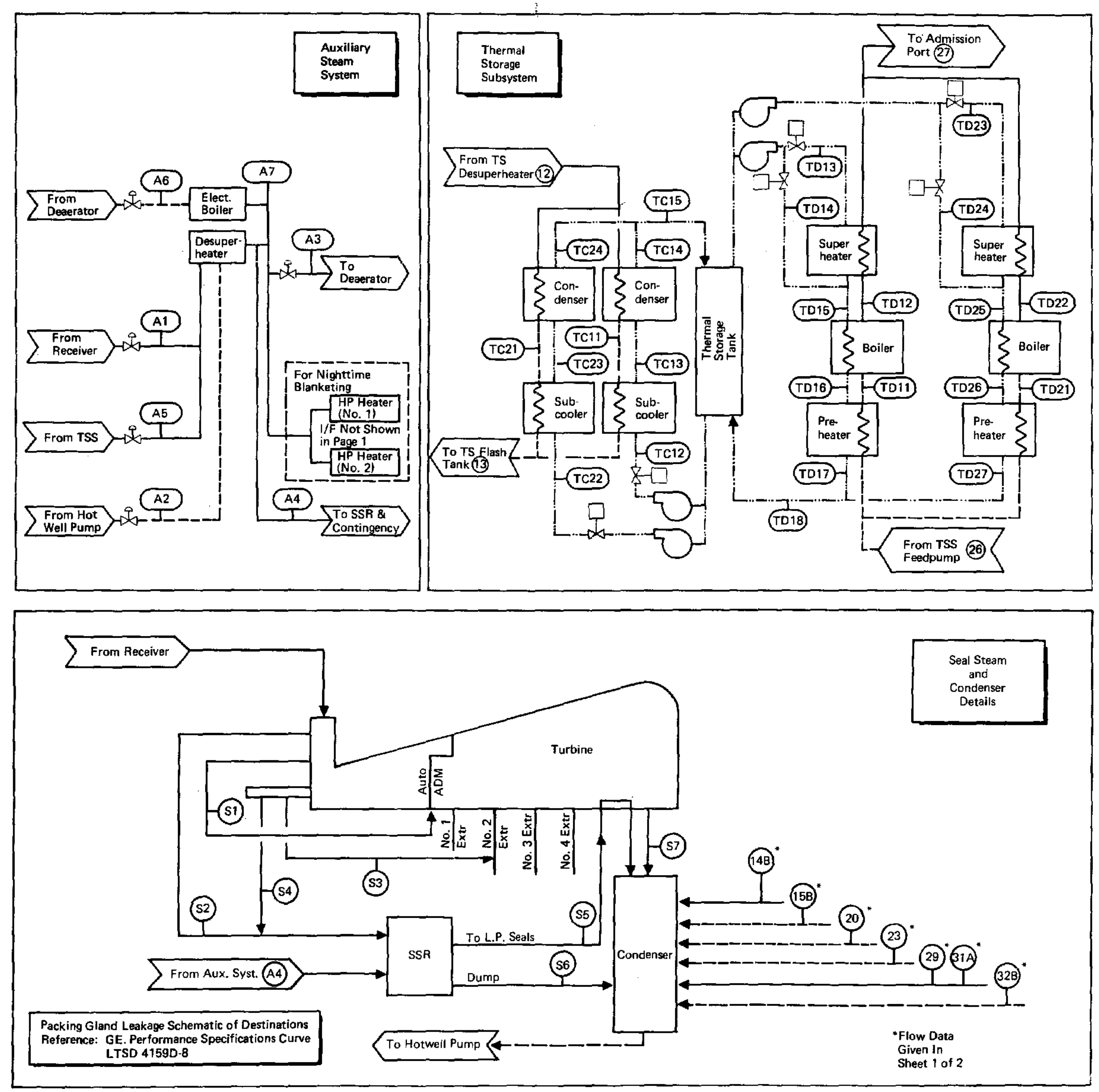

Legend

- Steam
- Feedwater/Condensate
- Thermal Storage Oil

Location Identification				Flow Rate (lb/hr)	Enthalpy (Btu/lb)	Temperature (°F)	Pressure (psia)
Auxiliary Steam System			A1				
			A2				
			A3				
			A4				
			A5				
			A6				
			A7				
Thermal Storage System	Charging Side	Train 1	TC11				
			TC12				
			TC13				
			TC14				
			TC15				
		Train 2	TC21				
			TC22				
			TC23				
			TC24				
	Discharging Side	Train 1	TD11				
			TD12				
			TD13				
			TD14				
			TD15				
			TD16				
			TD17				
			TD18				
		Train 2	TD21				
			TD22				
			TD23				
			TD24				
			TD25				
			TD26				
			TD27				
Seal Steam and Condenser			S1	1027.9	1461.0	960.0	1486.0
			S2	561.3	1461.0	960.0	1486.0
			S3	7885.2	1433.2	873.2	979.7
			S4	1099.7	1433.2	873.2	979.7
			S5	650.0	1442.6	818.9	15.7
			S6	1001.0	1442.5	818.9	15.7
			S7	77746.4	1000.5	108.7	1.228

DEPARTMENT OF ENERGY
SAN FRANCISCO OPERATIONS OFFICE

SOLAR TEN MEGAWATT PROJECT OFFICE
9550 FLAIR DRIVE, SUITE 210
EL MONTE, CALIFORNIA 91731

10 MWe SOLAR PILOT PLANT - DAGGETT, CALIFORNIA

SOLAR FACILITIES DESIGN INTEGRATOR

Rockwell International Rocketdyne Division

TITLE
HEAT AND MASS BALANCES
MODE 1-2

SCALE

DATE

DRAWING NO 4001003133901

SHEET NO 2 of 2

REV 1

REVISIONS

REFERENCE DRAWINGS

PRINT RECORD

Figure 3.3B. Heat and Mass Balance Mode 1 (10 MW Design Point)

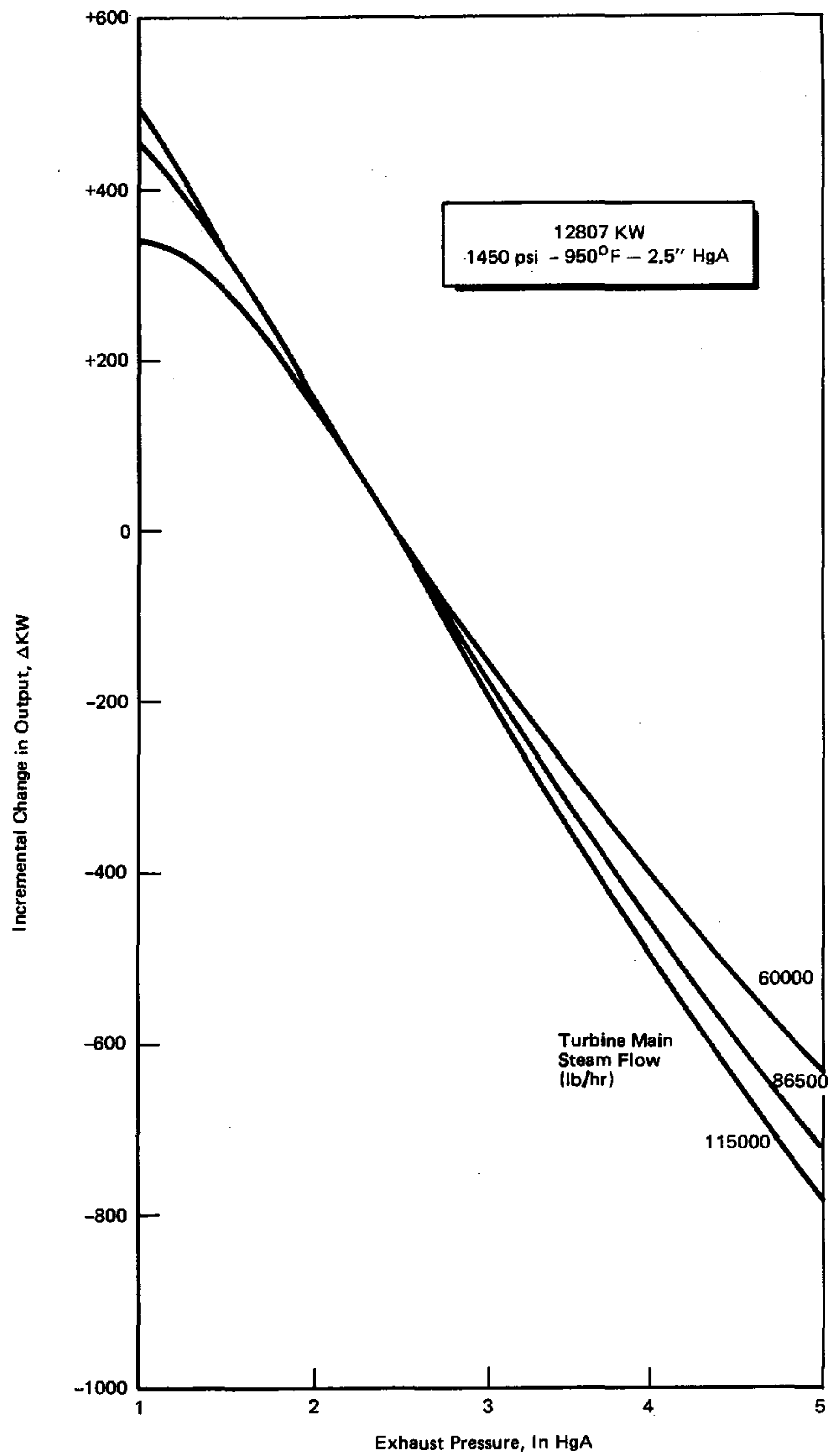

Figure 3.4. Impact of Turbine Exhaust Pressure on Electrical Output

Table 4.1. Mode 1 Plant Operating Data Base (Page 1 of 2)

Date	Day of Week	Online Period	Comment
12/25/82 (359)*	Sat	09:22 - 16:02	
1/10/83 (10)	Mon	10:28 - 16:10	Power step tests
2/1/83 (32)	Tue	10:48 - 16:38	
2/14/83 (45)	Mon	09:52 - 15:05	Off design temp and press
3/12/83 (71)	Sat	08:41 - 16:38	Midday clouds, steam dump valve leak thru
3/15/83 (74)	Tue	10:32 - 17:03	
4/9/83 (99)	Sat	08:42 - 16:27	Afternoon winds to 35 mph
4/16/83 (106)	Sat	08:44 - 17:30	
4/17/83 (107)	Sun	08:12 - 16:11	
4/18/83 (108)	Mon	07:29 - 12:23	Power step tests
5/7/83 (127)	Sat	09:46 - 18:46	Max power = 11.3 MWe gross
5/8/83 (128)	Sun	08:35 - 18:31	Afternoon winds to 30 mph
5/15/83 (135)	Sun	08:37 - 18:26	
5/21/83 (141)	Sat	08:21 - 14:42 16:24 - 18:40	High winds, midday trip (air system problems)
5/22/83 (142)	Sun	08:15 - 12:09 13:42 - 18:58	Midday trip (air system problems)
5/23/83 (143)	Mon	08:17 - 18:50	Air system problems
5/24/85 (144)	Tue	08:05 - 19:03	Air system problems
5/25/85 (145)	Wed	08:26 - 18:56	Air system problems
5/26/83 (146)	Thurs	10:09 - 18:58	Air system problems
5/27/83 (147)	Fri	08:30 - 18:47	Air system problems
5/29/83 (149)	Sun	08:44 - 17:49	Air system problems
5/30/83 (150)	Mon	07:42 - 19:04	Air system problems
6/2/83 (153)	Thurs	08:30 - 18:51	Air system problems

*Day of the year

Table 4.1. Mode 1 Plant Operating Data Base (Page 2 of 2)

Date		Day of Week	Online Period	Comment
6/6/83	(157)	Mon	08:50 - 16:44	Partly cloudy afternoon
6/9/83	(160)	Thurs	08:45 - 19:04	Hazy, low morning insolation
6/10/83	(161)	Fri	09:09 - 18:47	Hazy, low morning insolation
6/12/83	(163)	Sun	09:06 - 19:13	
7/7/83	(188)	Thurs	08:34 - 16:00	Power step test

Before reviewing the test results for Mode 1 operation, it is essential to understand both the overall philosophy associated with the instrumentation and data acquisition system as well as specific characteristics associated with particular instruments.

First and foremost, the plant is operated as a utility power plant as opposed to a precise laboratory experiment. As a result, the instrumentation used for the most part is of the type normally used in the process and utility industries. In addition, no dedicated pretest and post test calibration checks are made as would be done in a laboratory experiment to verify the quality of the data being recorded. As a result, uncertainties implicitly exist as to the absolute and relative accuracy of the data being recorded.

It should also be understood that the errors in the final data arise not only from the sensors themselves but from the entire data system through which the signals must flow. Most of the sensors used in the plant have accuracies typically on the order of 1/2 - 1% of full scale value. By the time the data signal is transmitted, processed, recorded, and retrieved, the accuracy may be more typically in the 2 - 2-1/2% range, even for precisely calibrated instrumentation. Factors in the data system which can contribute to the overall errors are the excitation power supplies, signal conditioning equipment, analog-to-digital converters, the precision of the digital system, and the calibration curves used to convert the digitized data into engineering parameters.

The maintenance of the instrumentation and data system represents a major task for plant maintenance personnel. With 3383* individual plant measurement tags contained in the Master Information File (2400 tags related to the Subsystem Distributed Process Control system, 744 tags dedicated to the engineering Data Acquisition System, and 239 tags associated with the Special Heliostat Instrumentation and Meteorological Measurement System), it is virtually impossible to conduct a periodic calibration check of all measurement channels within the limitations of the available manpower.

*A total of 1815 tags are currently scanned and recorded at any one time due to data base limits.

Table 4.2. Principal Mode 1 Process Instrumentation

Tag ID*	Description	Range
ATX1817A	Normal incident pyrheliometer (control room roof)	0-1394 w/m^2
TI2001P	Receiver inlet water temperature	0-500^oF
PI2002P	Receiver inlet water pressure	0-3000 psi
TI2005P	Receiver (boiler panel) inlet water temperature	0-800^oF
TI2904P	Receiver discharge steam temperature (RTD)	0-1200^oF
PI2902P	Receiver discharge steam pressure	0-2000 psi
FI2233P	Total receiver feedwater flow	0-208.5 klb/hr
PI1001P	Steam pressure at base of tower	0-1800 psi
TI1001P	Steam temperature at base of tower	0-1100^oF
JIC5100P	Gross generated electrical power	0-28800 KW
STX1801	Wind speed	0-100 mph
NE5102AP	Net generated electrical power	0-18417 KW
TI2903P	Receiver discharge steam temperature	0-1500^oF
TEX1102	Final feedwater temperature	0-450^oF
PI640P	Condenser pressure	0-12 In Hg Abs
TI115P	Feedwater temperature (inlet to 4th pt. heater)	60-200^oF
TI97P	Feedwater temperature (outlet to 4th pt heater)	0-250^oF
TI90P	Feedwater temperature (outlet from deaerator)	0-300^oF
TI40P	Feedwater temperature (inlet to 2nd pt. heater)	0-400^oF
TI13P	Feedwater temperature (inlet to 1st pt. heater)	0-500^oF
PE5001P	Plant electrical load	0-2800 KW
PI992P	Turbine first stage pressure	0-1500 psi

*See Figure 1.3 for Relative Location of Process Instrumentation

Instead, as deficiencies are noted by plant operators or engineering personnel, maintenance orders are written and corrective actions are initiated. Priorities in general are given to those parameters which directly involve the plant control system or those which monitor principal plant parameters for display in the control room. As a result, data which may be in error are continually recorded with no corrective action being taken until someone observes the problem and initiates the necessary corrective actions. Data of this type are of greatest concern for the more obscure parameters which are not widely reviewed on a routine basis. When a problem is observed, no effort is made to "correct" previously recorded data due to the uncertainty associated with when the problem originated.

Individual sensors in the plant also have unique preventive maintenance requirements which must be accomplished in order to afford reasonable measurement accuracy. For example, the alignment of the normal incidence pyrheliometer must be adjusted daily to insure proper alignment with the sun while dust on the lens, which will directly influence the measurement, must be cleaned away. Anemometers that are located at various points throughout the site to gather wind data, which can influence plant operation, must receive routine maintenance in terms of lubrication and bearing replacement. New bearings and fresh lubrication can significantly change the spinning resistance of the anemometer.

Finally, many critical sensors experience changes in output signals with operating conditions or tend to degrade with time. For example, flowmeters which are widely used in the receiver feedwater system (21 receiver flowmeters) tend to experience a zero point shift with operating temperature. Thus, as sensing elements change in temperature which occurs naturally as a result of normal variations in feedwater temperature, measured flow values are also directly affected. Flux sensors, which are integral part of the receiver control system, tend to experience a long term degradation in output signal with time. As a result, periodic surveillance of these signals is required and control system gain changes are necessary to offset these affects. Attempts are also made to periodically recalibrate these sensors to preserve the "engineering" quality of the data. However, since a standard calibration device is not available, the post calibration tests data still contain a great deal of uncertainty.

5.0 Test Results

This portion of the report presents the results of the Mode 1 test program. It is divided into three sections which cover steady state performance, transitions (startup and shutdown), and trips. Where appropriate, comparisons between the actual test data and the predicted design values are made to further enhance the meaning of the test data and to verify the quality of the assumptions and analysis used to develop the Solar One plant design.

5.1 Steady State Performance

The goal of this section is to present system level performance data for Mode 1 operation. The data cover both design and off design operating conditions. It is intended that these data provide insight as to the preferred operating conditions which maximize plant performance and net electrical power production.

In preparing the data for presentation in this report, the Mode 1 data base was sorted by critical parameters which can influence plant or system performance. Data pertaining to the water/steam portion of the system (including the turbine-generator cycle) was sorted by steam temperature and pressure. Data pertaining to the collector/receiver portion of the plant was sorted by steam temperature (indicative of receiver temperature), steam pressure, and wind speed. In all cases, data were screened to verify that a reasonably steady state condition existed before individual data points were selected for reporting purposes.

The system level performance and parametric sensitivity data for the water/steam portion of the plant are summarized in Figures 5.1 - 5.7. Figure 5.1 shows the gross electrical power production as a function of steam flow at two operating steam temperatures. It also shows the design relationship as specified in the GE Thermal Kit (see Reference 4) which is based on a steam condition of 950°F, 1450 psi and a condenser pressure of 2.5 in Hg. The high temperature data points (depicted as circles) show reasonable agreement to the GE performance predicted although the lower operating condenser pressures (0.6 - 1.4 in Hg) tend to result in a higher power for a given steam flow than would occur with a condenser pressure fixed at 2.5 in Hg.

The figure also shows, as expected, the higher steam flow required for low steam temperature operation (depicted as triangles). It is interesting to note that the high and low temperature data points tend to merge in the low

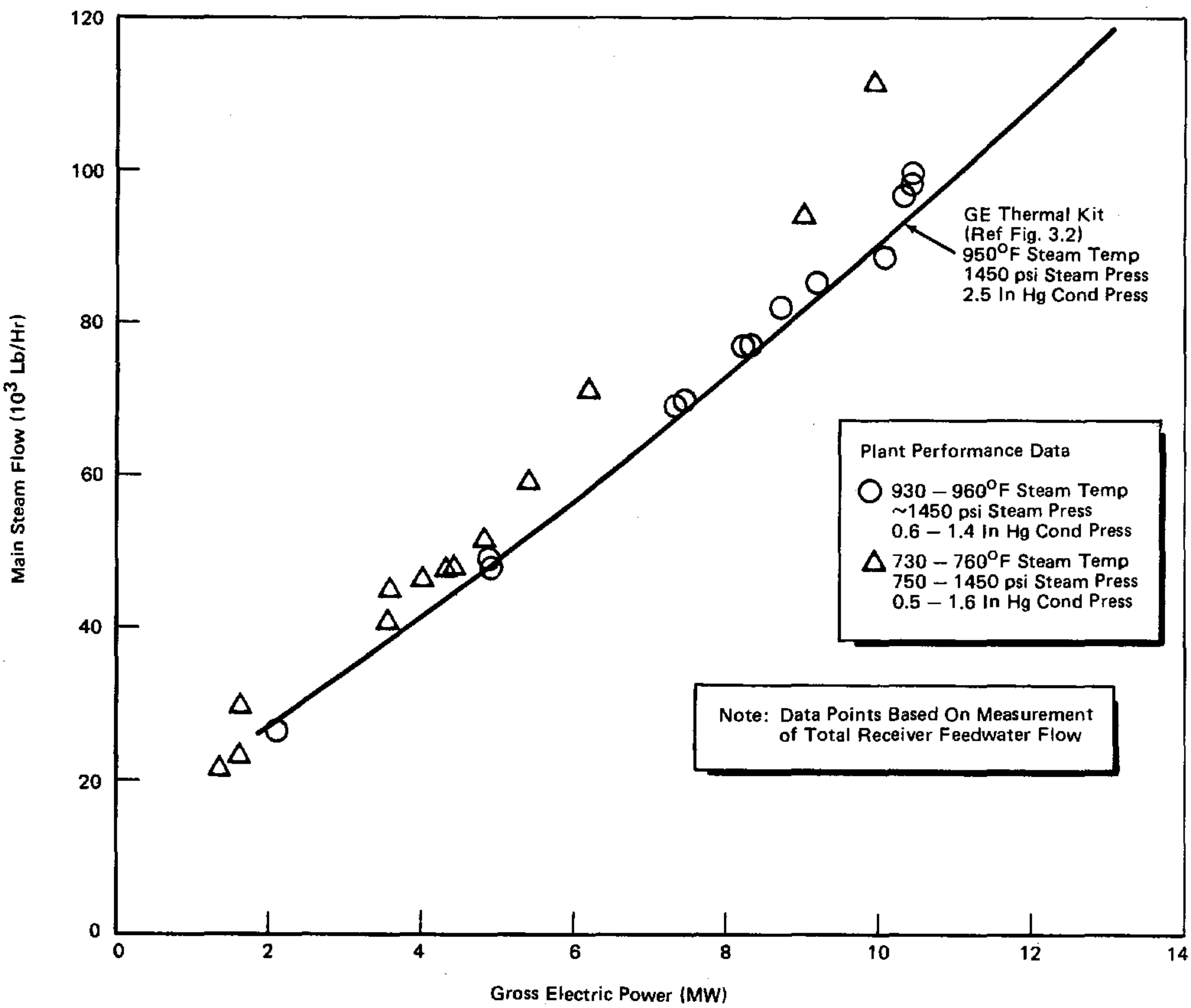

Figure 5.1. Main Steam Flow Required for Gross Electric Generation

power portion (left side) of the curve. From a turbine cycle standpoint, this implies that no significant advantage exists during low power operation in maintaining a high steam temperature. The fact that no distinguishable pressure affect was observed in plotting the low temperature data (low temperature data cover the pressure range of 750 - 1450 psi) indicates that pressure effects are of secondary importance to the relationship shown in the figure.

To make a direct comparison between the high temperature, high pressure data points (design point conditions) and the GE Thermal Kit prediction shown in Figure 5.1, the data were modified to "correct" the condenser pressure to the 2.5 in Hg design value. The basis of this correction was the "incremental change in electrical output" with turbine "exhaust" pressure shown in Figure 3.4. The resulting data comparison to the GE predictions are shown in Figure 5.2. Because the condenser pressure correction factors in all cases resulted in a reduction in gross electrical power generation for a given flow, the correlation between the predicted performance and the test data is not as good as was originally depicted in Figure 5.1, particularly at the high flow conditions.

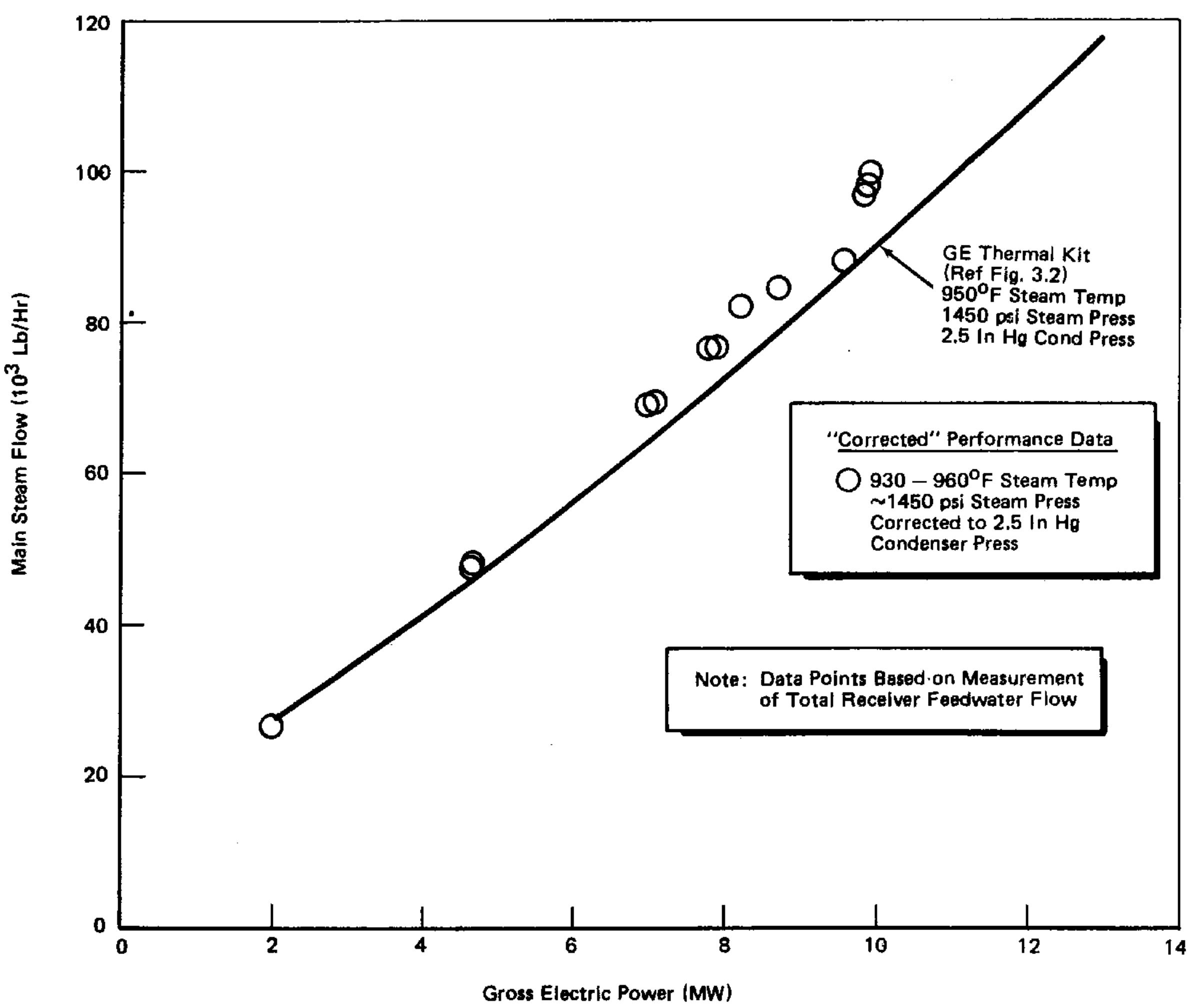

Figure 5.2. Performance Comparison Employing "Corrected" Condenser Pressure

The main steam flow data values shown in Figures 5.1 and 5.2 are in fact measured feedwater flow values at the inlet to the receiver. Some errors may exist between the feedwater flow and the steam flow which actually enters the turbine. Principal sources of these errors are the alternate steam flow paths which can consume some of the receiver-generator steam prior to reaching the turbine. These paths, which are shown in Figure 1.3, are the auxiliary steam system, the steam dump system and the bootleg drains. If substantial steam flow was being diverted to one or more of these paths, the most significant error would be observed in the low power region of Figure 5.2 since the lost steam flow would represent a substantial fraction of total steam flow. The fact that this condition does not exist indicates that the receiver feedwater flow is a resonable measure of total turbine main steam flow for Mode 1 operation.

An alternate steam flow measurement technique was investigated. This involved the correlation between turbine main steam flow and first stage exhaust pressure. Figure 5.3 shows the results of the comparison between two plant operating conditions and the GE predicted values. The figure shows that a substantial discrepancy exists between the predicted and measured values at low to moderate steam flows. The data points show a trend toward "0" pressure at "0" flow which seems much more realistic than the predicted minimum pressure of 375 psia at "0" flow. The figure also shows that the correlation varies with changing steam conditions even when steam pressure is held reasonably constant.

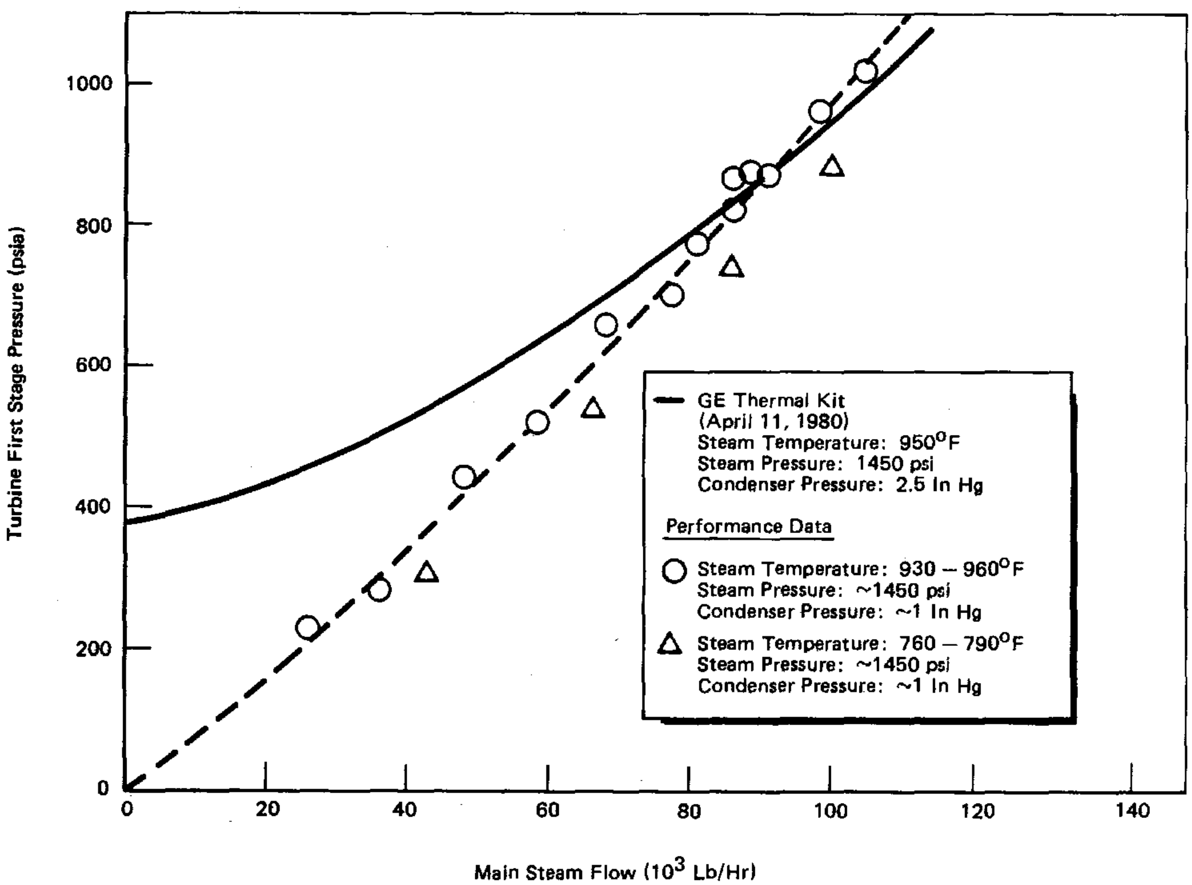

Figure 5.3. Comparison of Turbine First Stage Pressure to Main Steam Flow

As a result of the discrepancy between the predicted and measured values and the apparent need to have a unique first stage pressure versus main steam flow correlation for each steam condition, it was concluded that this technique would not give an accurate indication of turbine main steam flow. This would be particularly true due to the wide range of steam temperature and pressure conditions being evaluated in this report. Therefore, the receiver feedwater flow was adopted as a direct measure of turbine steam flow for this report and the related supporting analysis.

An indication of the water/steam cycle efficiency (expressed in terms of gross heat rate) is shown in Figure 5.4. This figure compares the calculated data points to the predicted gross heat rate as contained in the Heat and Mass Balance Analysis (see Reference 5). The experimental data have reasonable agreement with the predicted values. The data show that for power levels less than approximately 5MW, virtually no difference exists in the heat rates experienced for the high (930-960^{o}F) and low (730-760^{o}F) steam temperature. At higher power levels, the data indicate that the hot steam case (930-960^{o}F) is only marginally better than the low temperature case (730-760^{o}F).

Implicit in the performance of the overall water/steam cycle is the performance of the feedwater heaters which draw their energy from dedicated turbine extraction ports. Figure 5.5 shows a comparison of predicted and measured final feedwater temperatures as a function of gross electric power. The results show that the predicted temperature is consistently 5-10^{o}F higher than the measured data. The predicted values were developed prior to the selection of the feedwater heaters and ideal assumptions were made regarding the steam pressure drop through the turbine extraction steam lines. Further, the test data were taken with a condenser pressure of approximately 1 inch of Hg. As a result, the feedwater temperature leaving the condenser and entering the fourth point heater is 20-30^{o}F colder than the 108^{o}F initial feedwater temperature assumed for the Heat and Mass Balance Analysis.

Figure 5.5 displays data at four different steam conditions. It appears that the design steam conditions (shown as circles) result in a lower final feedwater temperature than is produced when the system operates at lower temperature and/or lower pressure steam conditions and at lower power levels. This effect is most likely related to the pressure drop that occurs across the turbine control values which are attempting to control upstream pressure. If the control values are maintained in a more wide open condition (as is the case for low steam pressure operation), the pressure drop across the valves will be less, which creates higher pressures at the turbine extraction ports and increased feedwater heating.

The performance of each of the four feedwater heaters at various power levels is shown in Figure 5.6. Predicted performance levels (dashed lines) are based on plant design steam conditions (950^{o}F, 1450 psi) and a 2.5 in Hg condenser pressure. The four large regions or zones formed by the dashed lines are the predicted zones of operation for each of the four feedwater heaters. The narrow zone which exists between the second and the third feedwater heater reflects the influence of the receiver feed pump on feedwater temperature due to the addition of mechanical pumping power.

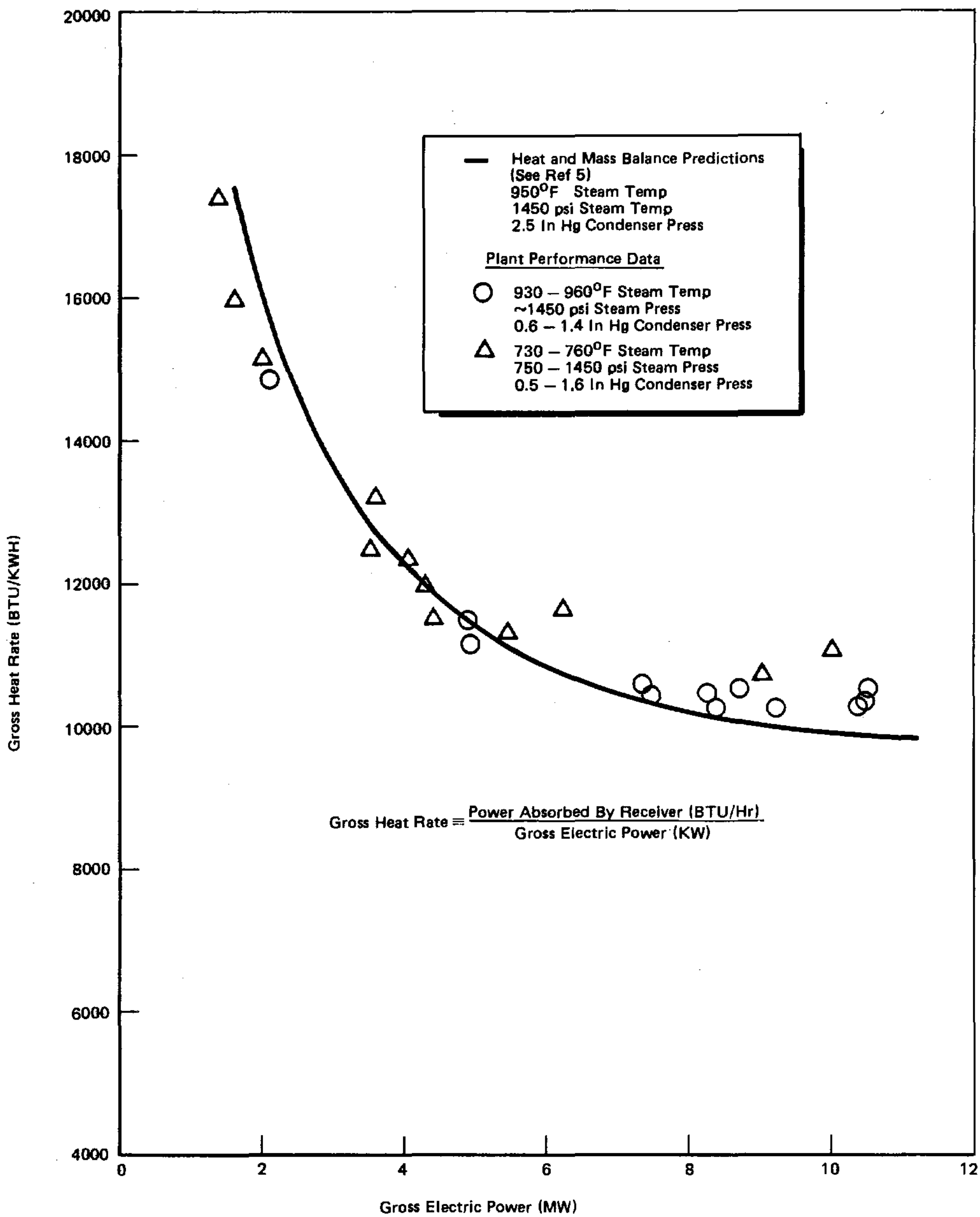

Figure 5.4. Gross Heat Rate for Water/Steam Cycle Portion of Plant

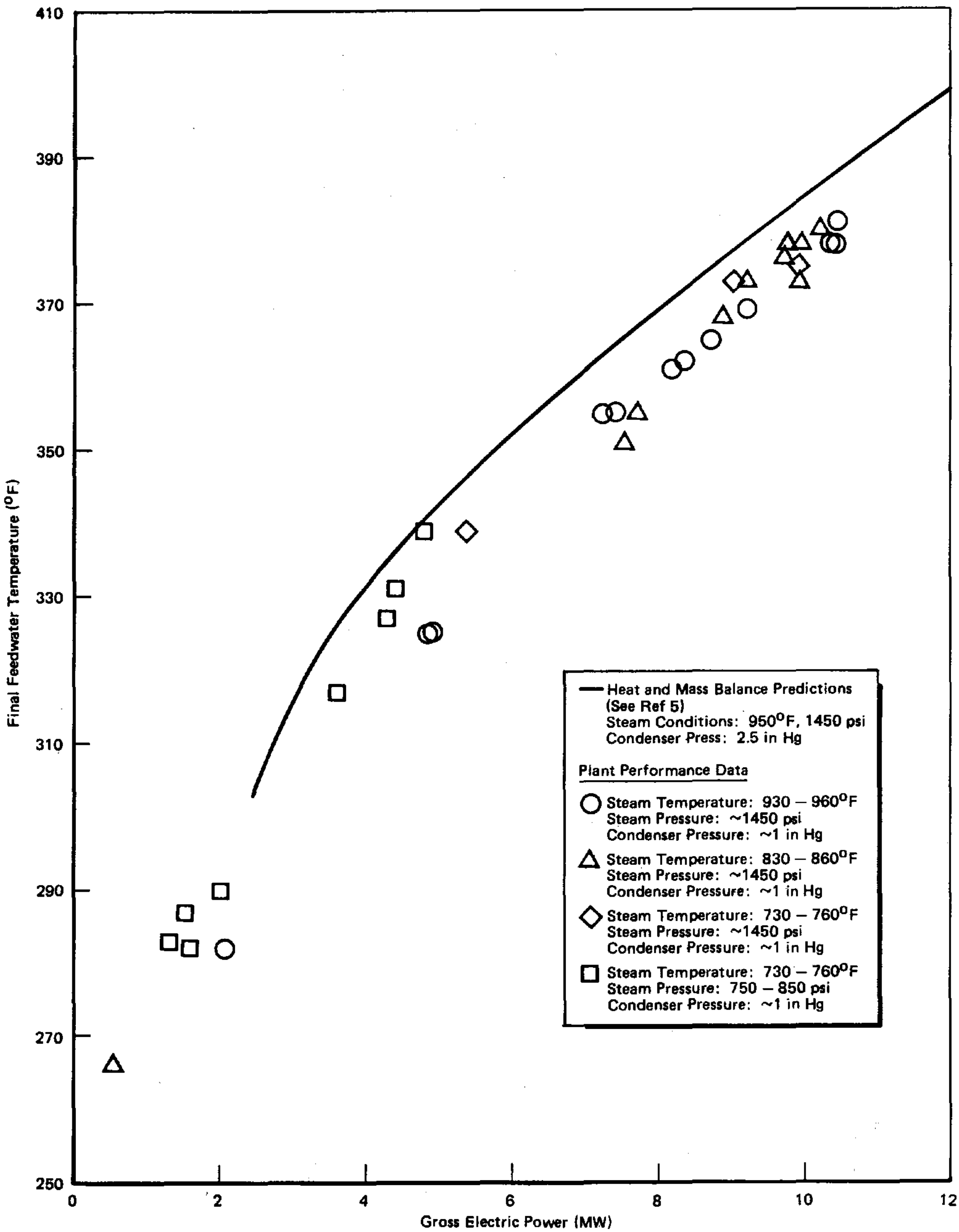

Figure 5.5. Variation in Final Feedwater Temperature

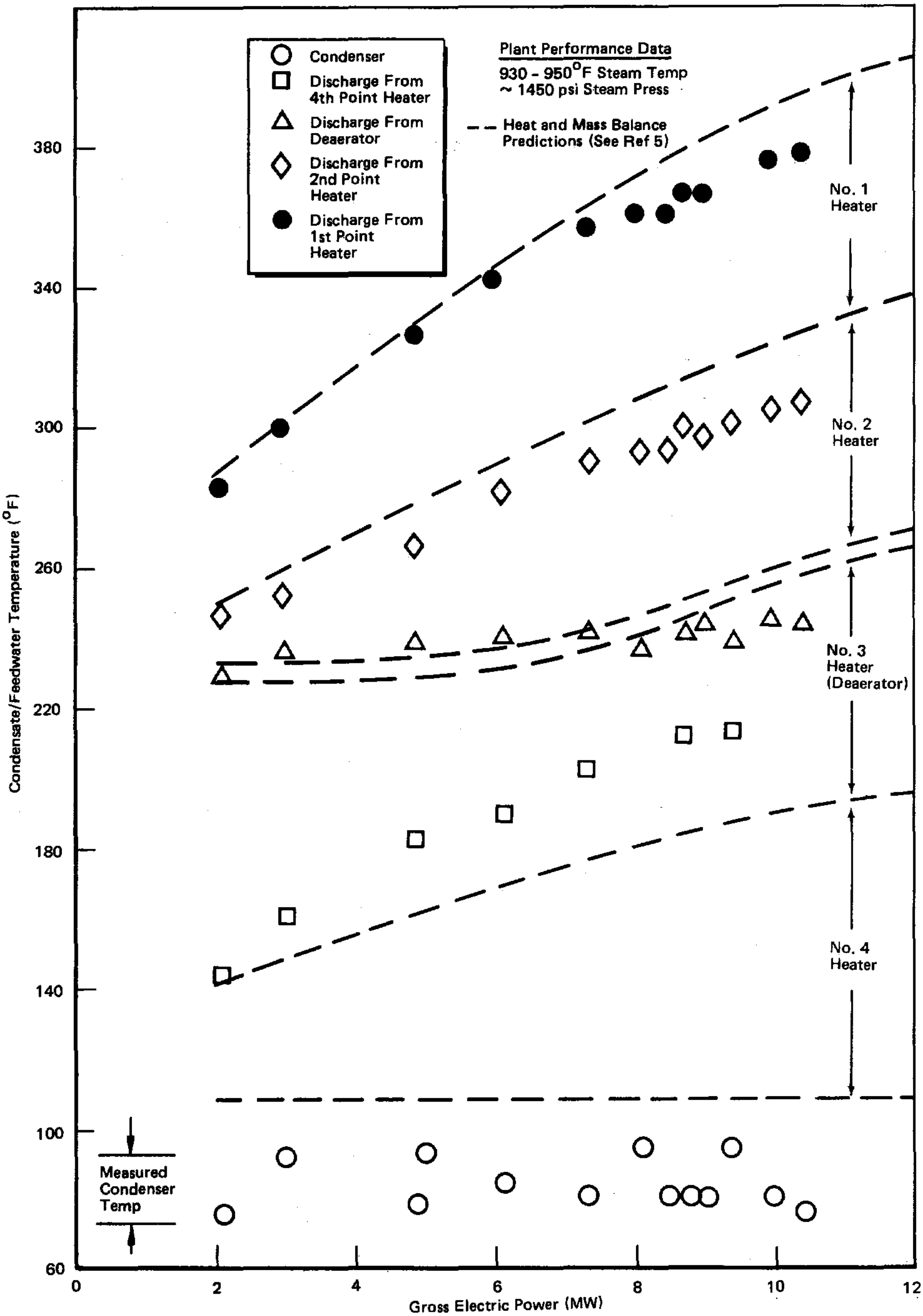

Figure 5.6. Performance of Individual Feedwater Heaters

The test data points plotted in Figure 5.6 correspond to similar steam temperature and pressure conditions as those assumed for the performance predictions. The influence of differences in condenser pressure between the test data and the 2.5 in Hg value assumed in the analysis are clearly seen at the bottom of the figure.

In comparing the test data to the predicted values, it is seen that the fourth point heater is assuming a greater portion of the feedwater heating than was originally predicted. The first and second point heaters appear to be providing a fraction of total feedwater heating which is comparable to original predictions while the deaerator is contributing a smaller than anticipated fraction to the total feedwater heating function. The net result for the entire turbine extraction and feedwater heater system however appears to be a more or less self compensating system in which adjacent heaters (and corresponding turbine extractions) tend to offset one another due to the highly coupled nature of the steam and feedwater flow paths. The result is that the final feedwater temperature approaches the predicted values reasonably well, particularly at lower power levels.

An additional performance factor which is heavily dependent on the operation of the water/steam cycle involves the plant parasitic load. Figure 5.7 shows actual parasitic load data as a function of gross electrical power for a variety of operating steam conditions. In general for high power operation, the plant parasitic load is between 1000 and 1200 KW, independent of the steam conditions involved. At lower power levels, the plant parasitic load decreases to approximately 1000 KW except for the case of reduced steam pressure operation (shown as squares). For this case, parasitic loads in the 800 - 900 KW range appear to be more appropriate due to the reduced power draw of the receiver feed pump. From the standpoint of parasitic load, the operation of the plant at reduced pressure offers a clear advantage. This operation is of course limited by the ability of the turbine and piping system valves to pass and control the steam flow without being "pegged" to a wide open (and non controlling) position. In all cases, the measured plant load (when the electric boiler was not in service) was significantly less than the 1700 KW load assumed for the plant design. The differences involve the extent to which plant electrical equipment is operated on a simultaneous basis during Mode 1 operation.

In order to complete the assessment of Mode 1 operation and to identify the preferred plant operating conditions, i.e., steam conditions, it is necessary to include the effects of the "solar" portion of the plant. Of critical interest are the effects of steam conditions on receiver performance. In addition, environmental factors such as wind speed can also influence the selection of receiver operating conditions.

For the purposes of this evaluation, the receiver can be treated as a "black box" whose absorbed power is given by:

$$P\ (\text{absorbed}) = P\ (\text{incident}) - (\text{Convective losses} + \text{Conduction losses} + \text{Radiation losses} + \text{Reflective losses}) \qquad (1)$$

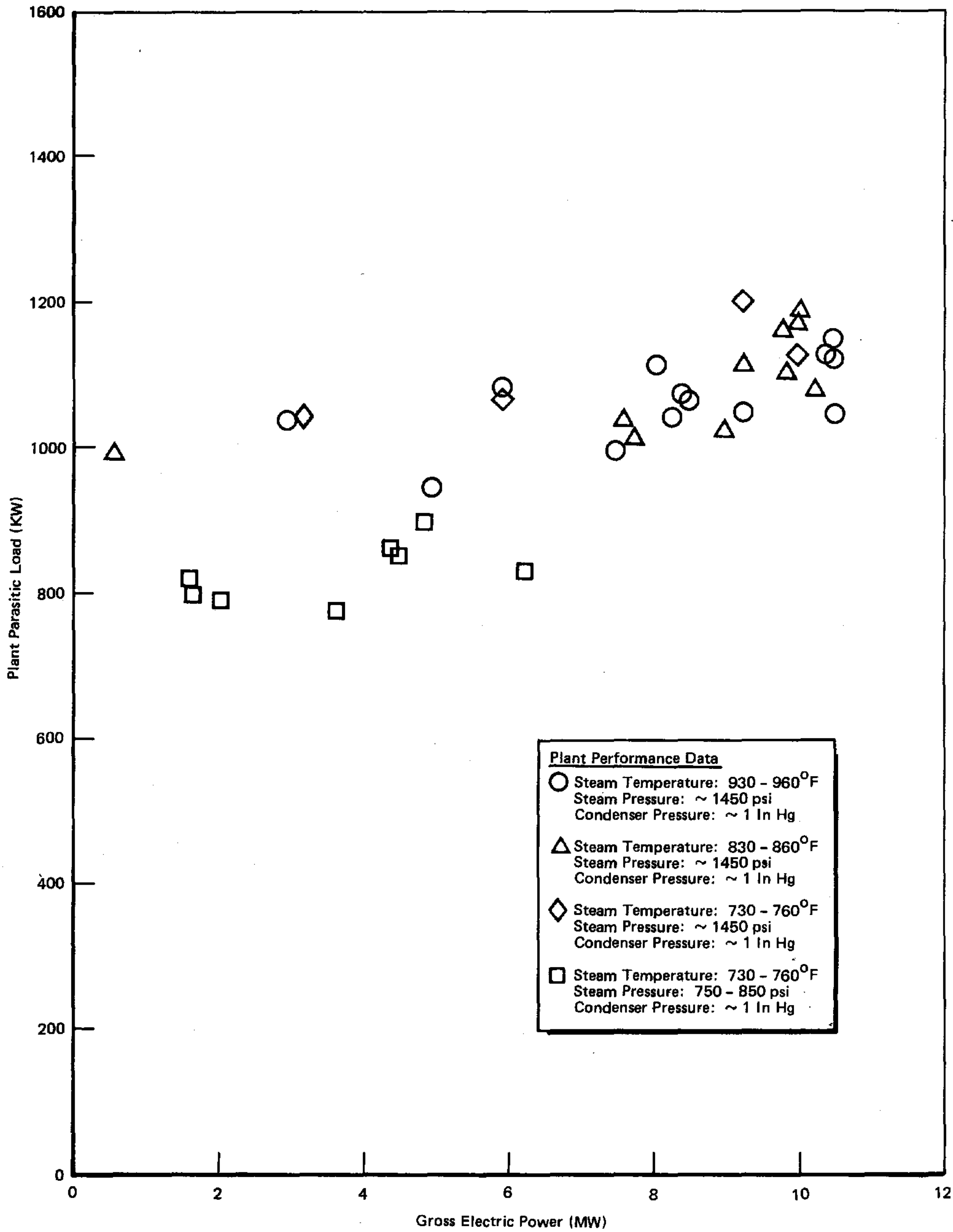

Figure 5.7. Measured Plant Parasitic Loads

The conductive losses are very small and can be neglected from the heat balance equation. The reflective losses are dependent upon the incident power and can be expressed as:

$$\text{Reflective losses} = (1 - \alpha) \cdot \quad P\,(\text{Incident}) \tag{2}$$

where

α - Receiver absorptance

Combining equations (1) and (2) and collecting terms yields in abbreviated form:

$$\text{Pabs} = (\alpha) \cdot \text{Pinc} - (\text{Conv loss} + \text{Rad loss}) \tag{3}$$

Using the basic "waterfall" efficiency parameters (see Figure 3.1), the incident power in turn can be expressed as:

$$\text{Pinc} = (\text{I})\,(\text{Cos})\,(\text{B \& S})\,(\rho)\,(\text{Atm Att})\,(\text{Rec Int})\quad(\text{Area Helio}) \cdot (\text{No Helio}) \tag{4}$$

where

I	- Measured direct insolation
Cos	- Average collector field cosine (See Table 3.2)
B & S	- Average collector field blocking and shadowing (See Table 3.1)
ρ	- Measured heliostat reflectivity
Atm Att	- Atmospheric attenuation
Rec Int	- Receiver interception factor
Area Helio	- Reflective surface area for an individual heliostat (39.59 m^2)
No Helio	- Number of heliostats tracking the receiver

Substituting equation (4) into equation (3), the power absorbed into the water steam can be written as

$$\text{Pabs} = (\alpha)\,(\text{Atm Att})\,(\text{Rec Int})\,(\text{Area Helio})\,(\text{I})\,(\text{Cos})\,(\text{B \& S})\,(\rho)\,(\text{No Helio}) - (\text{Conv Loss} + \text{Rad Loss}) \tag{5}$$

or

$$\text{Pabs} = K\,(\text{I})\,(\text{Cos})\,(\text{B \& S})\,(\rho)\,(\text{No Helio}) - (\text{Conv Loss} + \text{Rad Loss}) \tag{6}$$

where

K - Proportionality constant
= (α) (Atm Att) (Rec Int) (Area Helio)
(I) (Cos) (B & S) (ρ) (No Helio) - is a measure of the average power directed toward the receiver

If the proportionality constant and the convection and radiation losses are independent of receiver power, a plot of the test data based on equation (6) i.e., Pabs vs (I) (Cos) (B&S) (ρ) (No Helio) will result in a straight line relationship.

Test data for three different steam temperature ranges are plotted in Figures 5.8 - 5.10. The steam temperature ranges are respectively 930 - 960^{o}F, 830 - 860^{o}F, and 730 - 760^{o}F. In all cases, data selected represented steady state* plant operations with wind speeds less than or equal to approximately 10 mph. The steam pressures are as indicated in the figures.

The range of the data points on each figure reflect the typical operating ranges experienced during Mode 1 operation. The ranges for Figures 5.8 and 5.9 reflect plant operation to within approximately two hours of sunrise and sunset. Data shown in Figure 5.10 includes lower values of absorbed power and reflect plant operation to within approximately an hour of sunrise and sunset. It is seen in all cases, that a straight line relationship exists between the absorbed power and the power directed from the collector field toward the receiver, [(I) (Cos) (B&S) (ρ) (No Helio)].

With these data plots, it is possible to estimate receiver convection and radiation losses directly. Defining the following terms as

H = (I) (Cos) (B&S) (ρ) (No Helio)
L = (Conv Loss + Rad Loss)

equation (6) can be written in a simplified form as

$$\text{Pabs} = K\ H - L \qquad (7)$$

Differentiating equation (7) yields

$$d\ (\text{Pabs}) = K\ d\ (H) - 0 \qquad (8)$$

or

$$K = \frac{d\ (\text{Pabs})}{d\ (H)} \qquad (9)$$

*Steady state corresponds to clear day operations during which process set points and flow paths were held fixed for 15-30 min. Naturally occuring changes due to the diurnal sun motion occur on a continuous basis.

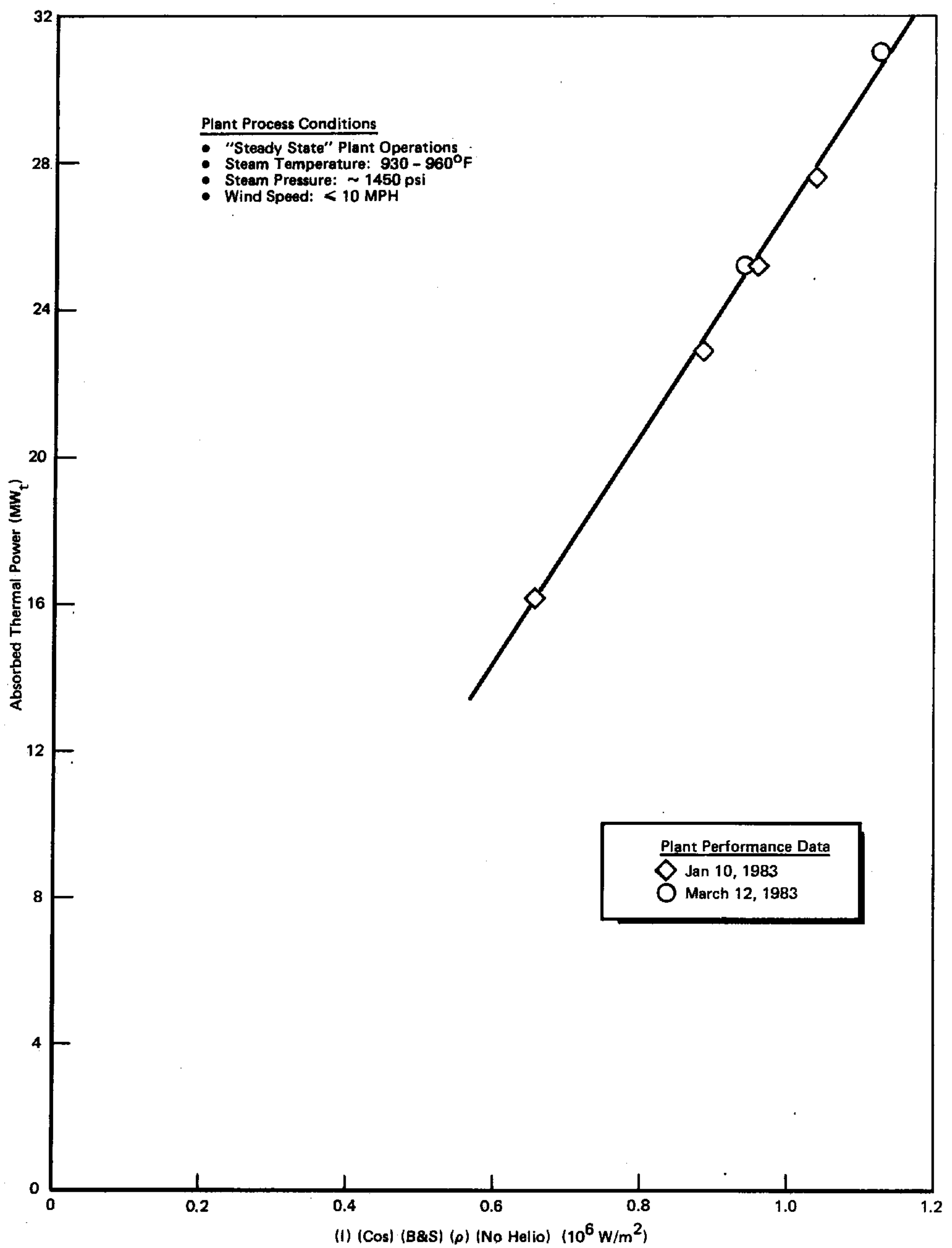

Figure 5.8. Receiver Absorbed Power as a Function of Collector Field Redirected Power (Steam Temp 930 – 960°F)

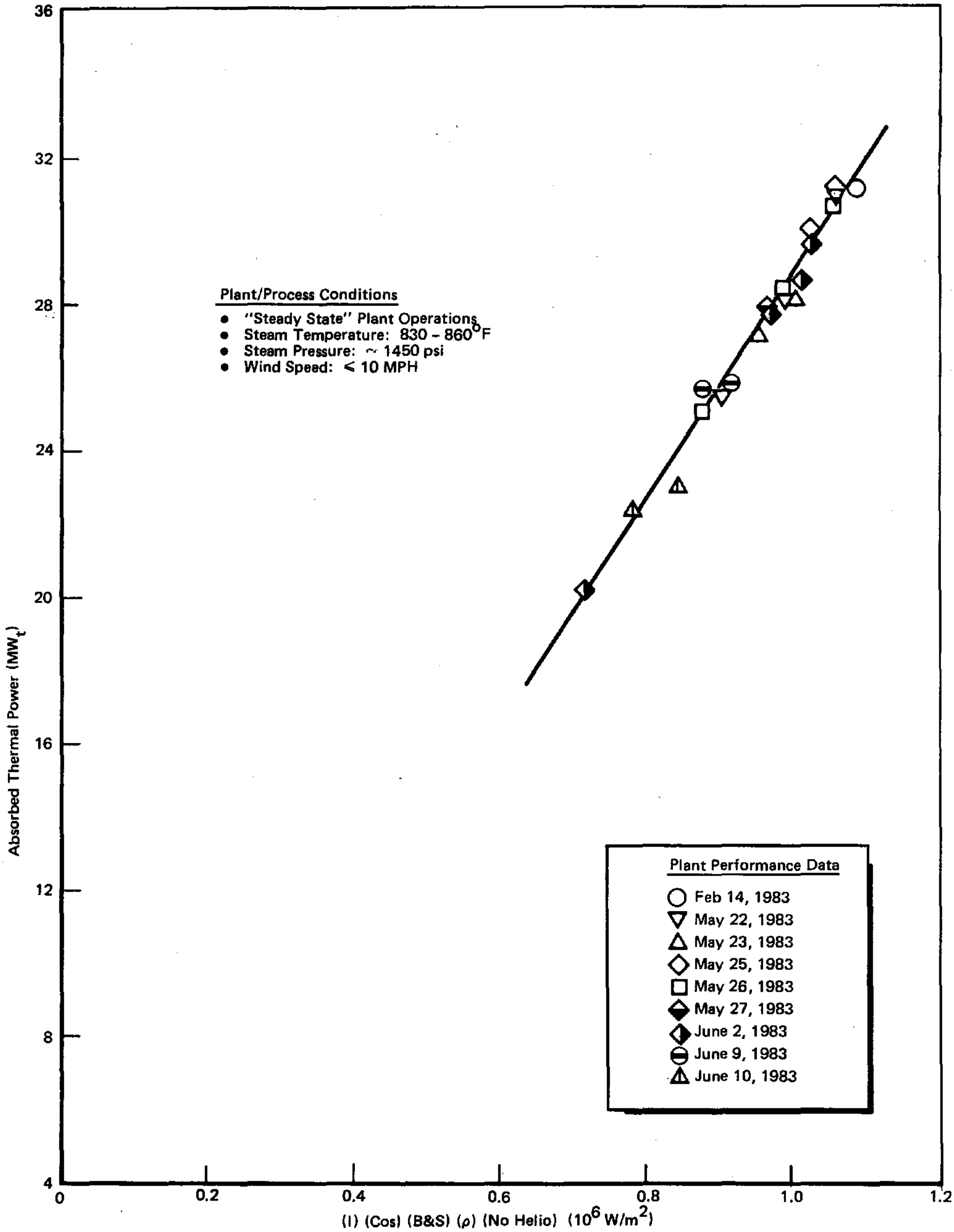

Figure 5.9. Receiver Absorbed Power as a Function of Collector Field Power (Steam Temperature 830 - 860°F)

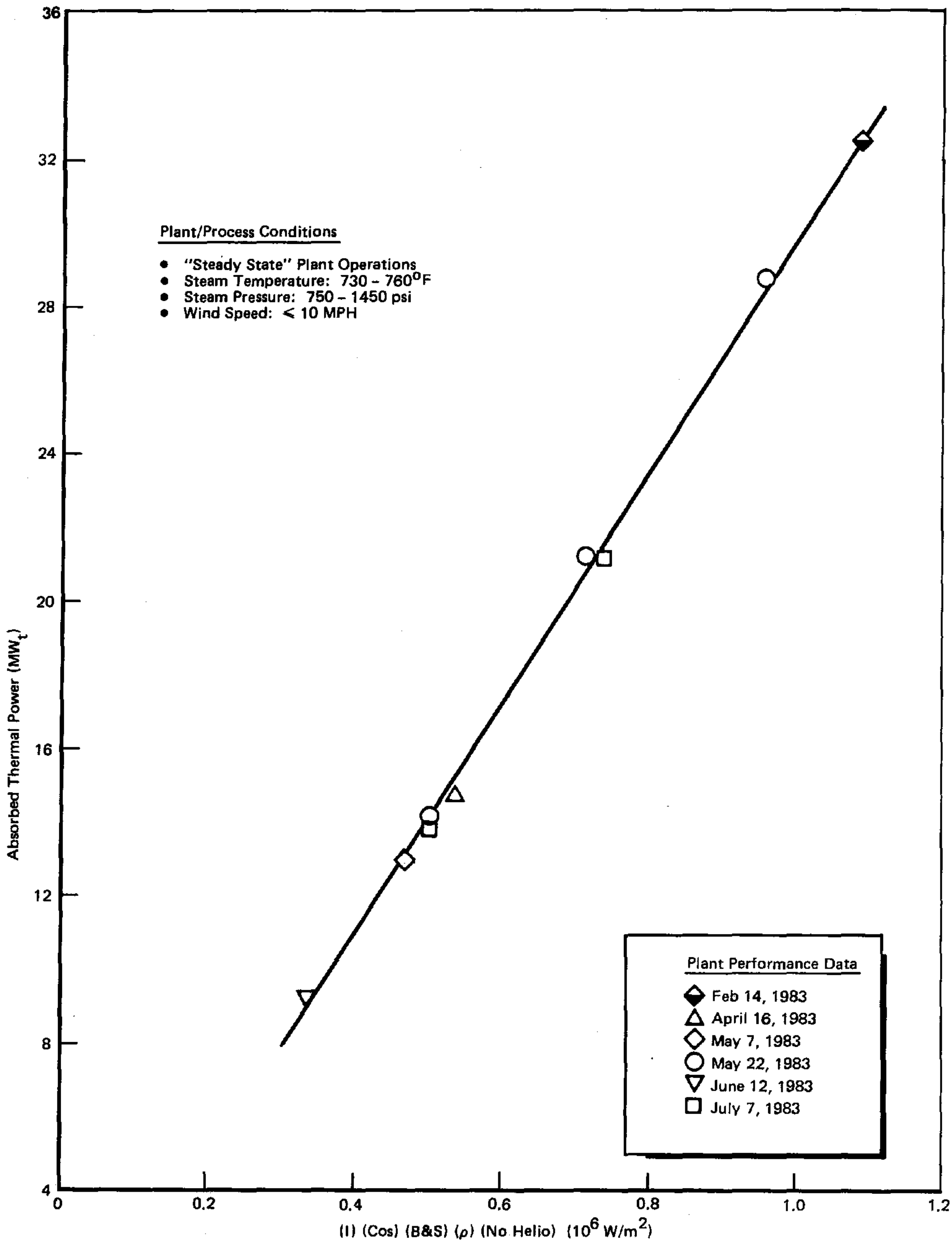

Figure 5.10. Receiver Absorbed Power as a Function of Collector Field Redirected Power (Steam Temp 730 – 760°F)

Since the data plots follow a straight line relationship, equation (9) can be written as the slope of the straight line formed by the data

$$K \triangleq \frac{\Delta\ Pabs}{\Delta H} \tag{10}$$

Substituting equation (10) into equation (7) yields

$$Pabs = \left[\frac{\Delta Pabs}{\Delta H}\right] H - L \tag{11}$$

By rearranging equation (11), the sum of the convection + radiation losses may be calculated directly from the relationship

$$L = \left[\frac{\Delta Pabs}{\Delta H}\right] H - Pabs \tag{12}$$

Using equation (12) and the straight-line slope data contained in each figure, the following receiver loss (convection + radiation) estimates were calculated. For comparison purposes, four reference case convection and radiation loss calculations are included. Cases 1 and 2 are appropriate to a 41 ft. tall receiver while cases 3 and 4 correspond to a 45 ft. tall receiver, identical to the Solar One receiver.

Test Data	Receiver Steam Conditions: Steam Temp	Receiver Steam Conditions: Steam Press	Wind Speed	Estimated Conv + Rad Losses
Figure 5.8	930-960°F	1450 psi	< 10 mph	4.11 MW_t
Figure 5.9	830-860°F	1450 psi	< 10 mph	1.97 MW_t
Figure 5.10	730-760°F	750-1450 psi	< 10 mph	1.65 MW_t
(Reference Calculated Losses)				
Case 1*	960°F	1450 psi	8 mph	4.2 MW_t
Case 2*	660°F	1450 psi	8 mph	3.27 MW_t
Case 3**	960°F	1450 psi	8.5 mph	4.66 MW_t
Case 4**	960°F	1450 psi	14.5 mph	4.92 MW_t

*From Reference 6
**From Reference 7

A comparison between the loss estimates based on the test data and those determined through traditional analytical techniques show reasonable agreement for operation at high steam temperature. Comparisons for lower temperatures show that the loss estimates based on test data are significantly lower than those analytically determined (Reference Case 2).

At this point, it is possible to combine the "solar" and water/steam cycle performance characteristics into overall plant level performance factors which can be used to determine the optimum plant operating conditions. Figure 5.11 shows a plot of the gross electric power generated by the plant as a function of the collector field redirected power parameter [(I) (Cos) (B&S) (ρ) (No Helio)]. The data points are all at steady state plant operating conditions for wind speeds less than approximately 10 mph. The specific steam conditions are indicated by the symbols.

In order to maximize plant output, steam conditions should be selected which result in the highest gross electric power generation for a given value of the collector field redirected power parameter. Of the data cases shown in Figure 5.11 the "open diamonds" exhibit this trait more than any other data case. The steam conditions corresponding to this case are 730-760^{o}F and 750-850 psi. This somewhat surprising result differs significantly from the 950^{o}F, 1450 psi plant operating design point. The preference for low temperature, low pressure operation is most pronounced at low power levels. At higher power levels, the low temperature operating points tend to merge with the intermediate temperature data points (830-860^{o}F - "triangular" data points). In all cases shown, the design point data ("circular" data points) appear to be less preferred.

The preference for lower than design temperature and pressure operation is even more apparent when the data is plotted in terms of net electrical power supplied to the grid as a function of the collector field redirected power parameter as shown in Figure 5.12. The lower pressure operating points ("diamond" data points) are relatively higher on the plot than the other data points due to the lower parasitic pumping power (receiver feed pump) consumed during low pressure operation.

Physically, the preference for operation at reduced steam pressure and temperature conditions, as shown in Figure 5.11 and 5.12, is a result of four factors which operate simultaneously during plant operation. These factors are the influence of steam conditions on turbine cycle efficiency, the influence of mass flow on turbine system performance, receiver heat losses, and plant parasitic electrical loads.

The influence of steam conditions on turbine cycle efficiency was shown in Figure 5.4. This figure showed that high steam temperature operation was slightly superior at high power levels but virtually no difference existed for power levels less than 5 MWe. Thus for the particular turbine used at Solar One, only a minor dependence of steam temperature on cycle efficiency exists.

From the standpoint of mass flow, the lower steam temperature results in a higher mass flow. This tends to cause the turbine to operate at higher (more near design) flows which is close to design point expansion efficiencies. In addition, the higher steam flows also cause the turbine main steam inlet control valves to operate in a more wide open position thereby minimizing losses across the control valves. This benefit is further enhanced by operating at reduced pressure where the control valves approach a full open condition. In order to allow for realistic upstream pressure control (normal control mode), the steam pressure and/or temperature should not be degraded below design conditions any further than the conditions compatible with the turbine control valve being 85-90% full open. Continued reductions in

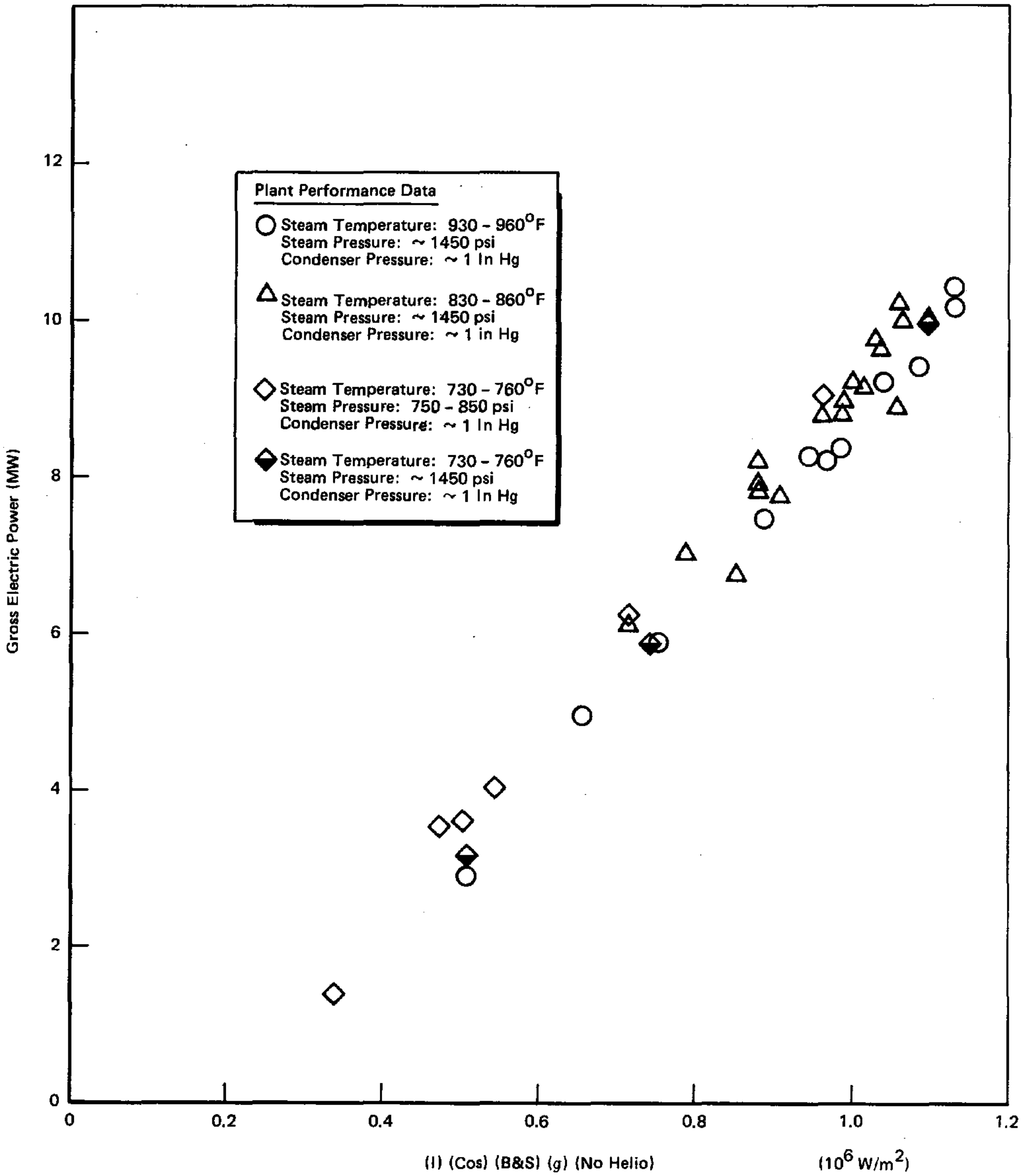

Figure 5.11. Gross Electric Power as a Function of Collector Field Redirected Power Parameter

temperature and pressure set points below that level would result in the turbine control valves going full open with a corresponding loss in pressure control. During the normal afternoon reduction in available solar power, further reductions in steam temperature and pressure are possible and desirable to enhance performance and reduce control valve losses.

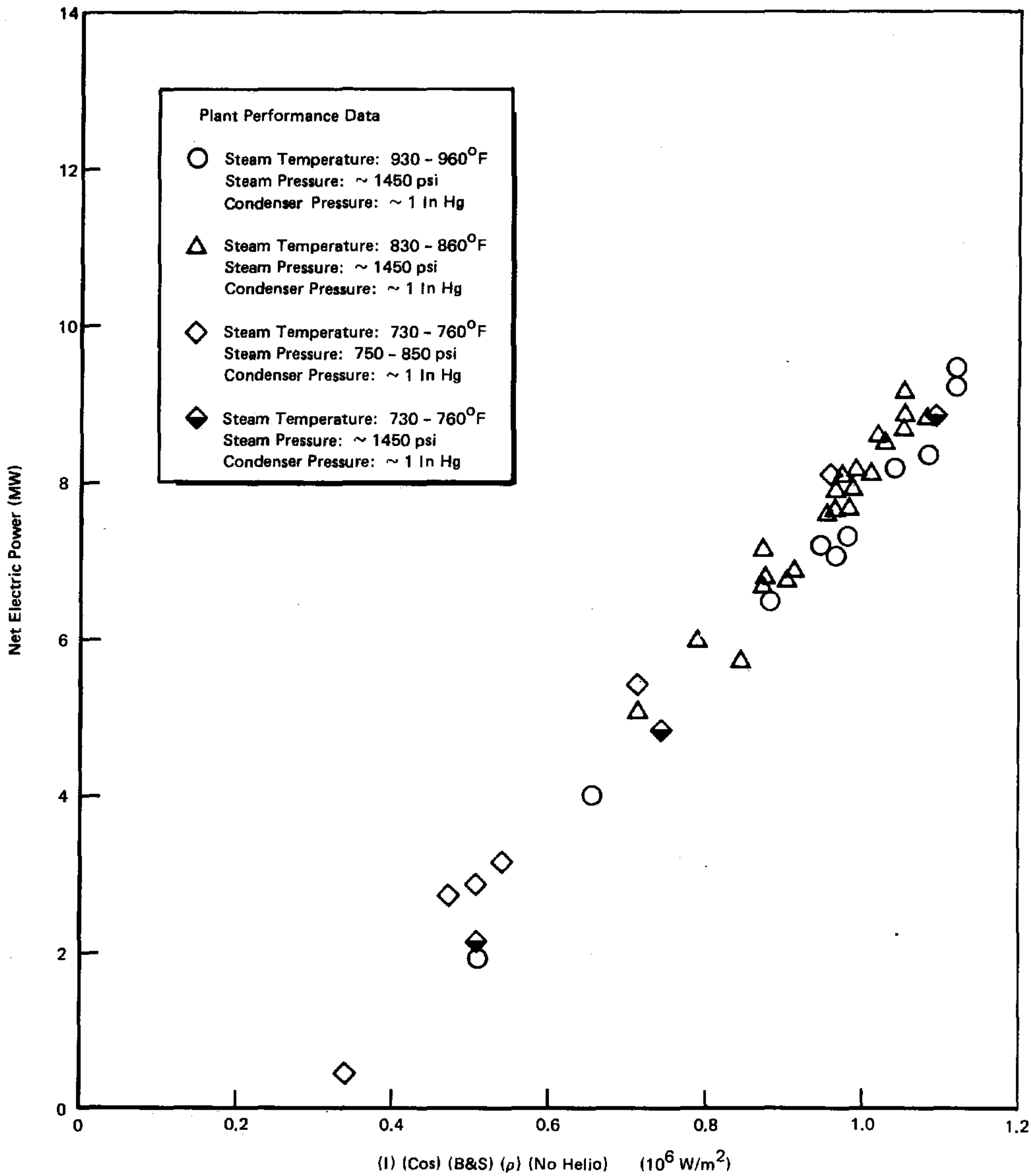

Figure 5.12. Net Electric Power As a Function of Collector Field Redirected Power Parameter

From the standpoint of receiver heat loss, the data shown in Figure 5.8-5.10 and the accompanying summary heat loss table showed the desirability of operating the receiver at lower than design steam temperatures. Since these data are all for low wind conditions, it can be argued that high wind operation would further enhance the relative performance benefits to be realized by low steam temperature operation.

From a parasitic power standpoint, Figure 5.7 showed that a parasitic load reduction of approximately 200 KW can be realized by operating at reduced system pressure. This saving is primarily associated with savings in receiver feed pump power.

One major portion of the Mode 1 test objectives which remains to be demonstrated involves the 4 and 7.8 hours durations for greater than 10 MWe net power generation on winter and summer "design" days respectively. Several factors have contributed to the inability to demonstrate these test objectives. These factors involve the available insolation, heliostat reflectivity and heliostat availiability.

Throughout the course of the test program, measured insolation levels have been significantly less than the "Design Day" values shown in Figure 2.1. Typical insolation deficiencies are on the order of 10-15%. This deficiency is of critical importance during the beginning and ending periods of the time intervals involved since no surplus generating capability exists at those points in time. This is in contrast to operations around solar noon when the deficiency in insolation and other factors is more than offset by the increased collector field output resulting from improvements in field cosine and blocking and shadowing factors.

The second factor that has resulted in reduced plant output is heliostat reflectivity. With the plant designed for an 0.89 reflectivity, this corresponds to a field with a 98.2% cleanliness factor relative to the field average 100 percent "clean" reflectivity factor of 0.906. Heliostat reflectivity measurements indicated that typical cleanliness factors of 90-95% of clean (0.815 to 0.860 reflectivity) were more representative of conditions which existed during the Mode 1 test program.

Heliostat outage is the third factor which influences power generation capability. The plant design point was based on having all 1818 heliostats tracking the receiver. Typically during the course of the Mode 1 testing, 2-3% of the heliostats were out of service. As a result of intensive heliostat maintenance activities, this outage level was reduced to approximately 1% by early summer of 1983.

The overall affect of the above three factors is to reduce the instantaneous plant power output by typically 15-20%. This of course directly affects the ability of the plant to demonstrate a design power output level for a specified time interval.

5.2 Transitions Involving Mode 1 Operations

The principal transitions of interest involving Mode 1 operation are plant startup and shutdown.

Plant startup can be categorized in terms of sunrise or early morning and midday startups. For the sunrise or early morning startup case, a condition exists where there is a deficiency in collector field power relative to what is required to start the receiver. In general, the deficiency is greatest on the east side (sun side) of the receiver where early morning heliostat performance is poorest.

The normal procedure during a sunrise or early morning startup is to command all of the available eastside heliostats to track the receiver. A lesser portion of the north and westside heliostats track those portions of the receiver in order not to overwhelm the receiver startup flash tank with steam flow (flash tank flow rated at 1/3 maximum receiver design flow -- 40,000 lb/hr) while waiting for the eastside of the receiver to reach steaming conditions. Collector field related factors which tend to extend early morning startup times are low early morning insolation and low performance associated with field cosine and blocking and shadowing losses. Other early morning factors which also influence startup times are dew or frost on the heliostats which significantly reduce or inhibit heliostat reflectivity. These latter two factors may delay startup as much as 30 to 45 minutes depending on their severity and the rate at which it melts and/or evaporates.

Midday startup conditions are those periods during which the collector field has an excess power capability relative to what is required to start the receiver. In general, all clear day startups initiated later than 2 hours after sunrise are of the midday type. During these periods, the rate at which heliostats are commanded to track are limited by the receiver executing its predefined startup sequence while maintaining reasonable control of process conditions once steaming operation is reached (minimize large temperature overshoots as superheated steaming conditions are reached). Again, collector field redirected power must be adequately managed so as not to overwhelm the receiver flash tank with steam flow from highly powered panels while awaiting the lower powered panels to reach superheated steaming operation.

Table 5.1 shows some typical startup timeline data for both sunrise and midday starts. The table shows that typically 1 1/2 - 1 3/4 hours are spent during a sunrise start producing a receiver steaming condition and establishing steam flow to the downcomer. Corresponding receiver startup numbers shown in the table for midday starts are 25 - 42 minutes. The difference is the ability of the collector field to deliver power to the receiver. Experience during sunrise starts has shown that the field may be "defocused", a problem may be corrected, and the startup group commanded back to "track" during the first 30 - 45 minutes following sunrise with virtually no impact on the overall startup time. Thus it can be concluded that the available power from the collector field during the period of 30 - 45 minutes immediately following sunrise contributes little in starting the receiver. As the sun elevation increases however, simultaneous increases in the insolation and field cosine and blocking and shadowing factors dramatically increase the redirected power from the collector field resulting in a substantial improvement (decrease) in receiver startup time.

The other data contained in Table 5.1 reflect the time required to prepare for turbine roll once downcomer steam is established and the time required to accelerate the turbine to synchronous speed and synchronize the generator. The activities required prior to turbine roll involve establishing superheated conditions (50^{o}F superheat) upstream of the main steam stop valve, warming the turbine steam chest, and completing preroll tests and checks. Following turbine roll, a time period is required to accelerate the turbine and accomplish the 1000 RPM hold in accordance with the GE turbine instructions as well as carrying out final checkout prior to synchronization.

Table 5.1. Mode 1 Startup Timelines (Clock Times)

Date	Start Tracking Receiver	Steam to Downcomer	Turbine Roll	Plant Online	Elapsed Time
(Sunrise Starts)					
3/12/83	6:06	7:38	8:14	8:41	2 hr 35 min
4/2/83	5:37	7:12	7:34	7:50	2 hr 13 min
4/4/83	5:34	7:05	7:35	7:52	2 hr 18 min
4/7/83	5:30	6:53	7:27	7:48	2 hr 18 min
4/13/83	5:22	7:05	7:37	7:59	2 hr 37 min
4/18/83	5:16	6:55	7:12	7:29	2 hr 13 min
4/19/83	5:14	6:52	7:14	7:31	2 hr 17 min
(Midday Starts)					
1/10/83	13:05	13:38	14:24	14:38	1 hr 33 min
1/11/83	11:03	11:45	12:00	12:13	1 hr 10 min
3/9/83	8:00	8:25	---	9:30	1 hr 30 min

Following synchronization, the turbine is partially loaded and then transferred to initial (upstream) pressure control. At that point, all remaining standby heliostats are commanded to track the receiver while the turbine control valves are used to ramp system pressure to the final desired operating value.

This transition and turbine loading sequence is shown at the extreme left side of Figure 5.13. The figure documents five parameters for a 600 minute period starting at 8:00 a.m. on day 144 (5/24/83). The parameters are:

FI2233 - Total receiver flow (klb/hr)
PI1001 - System control pressure (psi)
TI2904 - Receiver discharge steam temperature (^{o}F)
ATX1817A - Direct insolation (w/m^2)
JIC5100 - Gross electric power generated (kw)

The full ranges as well as the line symbols for each parameter are also shown on the figure. As shown by the figure, the actual turbine loading sequence, transfer to pressure control, and pressure ramping occur over approximately a 20 minute period. The slight increase in generated power over the period from approximately 40-60 minutes reflects both the naturally occurring power rise associated with morning operation plus the activation of the turbine extraction for feedwater heating.

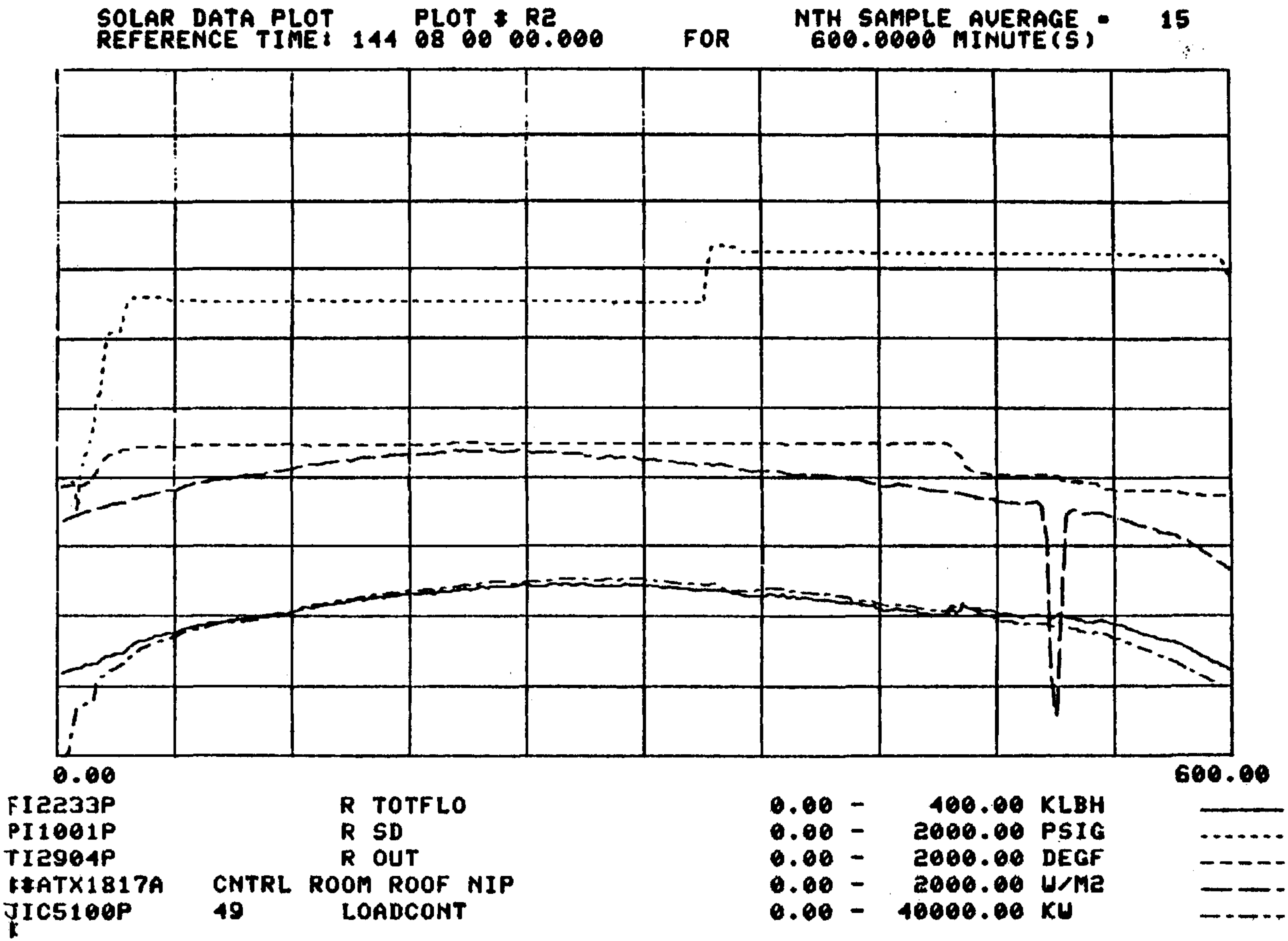

Figure 5.13. Major Mode 1 Plant Parameters, Day 144 (5/24/83) 08:00 – 18:00 Hrs

Figure 5.13 also shows plant operating traces for a typical clear day. The electrical power generation line tends to naturally follow the measured direct insolation. The trends show that once the initial synchronization and turbine loading activities were complete, the operator made only one change to major process operating conditions prior to the 450 minute point. This change (at the 350 minute point) involved a simple set point change in which the system presure was raised from 1300 to 1450 psi.

As the afternoon proceeded (beyond the 450 minute point in Figure 5.13), the operator begins to make a series of adjustments to the system temperature and pressure set points in an effort to prolong plant operations. Temperature set point reductions are aimed at maximizing the receiver flow thereby improving controllability of the 18 individual boiler panels as total power decreases. The short term reduction in measured insolation shown in Figure 5.13 at approximately the 500 minute point results from an antenna shadow which passed over the normal incident pyrheliometer. As shown in the figure, this event had no significance on plant operation.

Figure 5.14 shows an expanded view of major plant parameters during the final 2 hours of operation on day 144 (5/24/83). The period shown is from 17:00 to 19:00 hours with the 18:00 hour point being a direct continuation of the data lines shown at the extreme right edge of Figure 5.13. This figure shows the pressure and temperature set point adjustments that were made prior to removing the turbine generator from the line. Conditions immediately prior to going off line (shown at the right side of Figure 5.14) are 655 psi, 675^{0}F with a generator output of 588 KW which is less than 5% of the 12.5 MW turbine generator rating. On this day, the unit was taken off line at 19:03 with sunset occurring at 19:45.

5.3 Trips

The two types of trips of interest as part of Mode 1 testing are trips of the turbine with continuing receiver operation and trips of the receiver which shutdown the operation of both the receiver and the turbine. The data base developed for each of these trips is based on actual trip events which occurred in response to process upsets or equipment failures.

The typical system behavior in response to a turbine trip is shown in Figure 5.15. This figure represents a 10 minute time slice during which a turbine trip occurred at slightly more than 7 minutes into the plot (as shown by the rapid fall off in electrical power - JIC5100). Following the trip, steam pressure control was automatically assumed by the steam dump system and the pressure set point was reduced from 1400 psi to 1000 psi. During and following the turbine trip, the receiver operation continued in an uninterrupted fashion as indicated by the stable and continuing data traces associated with total receiver flow (FI2233) and receiver discharge steam temperature (TI2904).

The typical system behavior in response to a receiver trip is shown in Figure 5.16. This figure represents a 30 minute time slice during which a receiver trip due to high inlet water pressure occurred midway through the period. The plot shows the rapid increase in feedwater pressure (PI2002) which initiated the trip along with the rapid falloff in electric power (JIC5100), receiver flow (FI2233), and steam pressure (PI1001) immediately

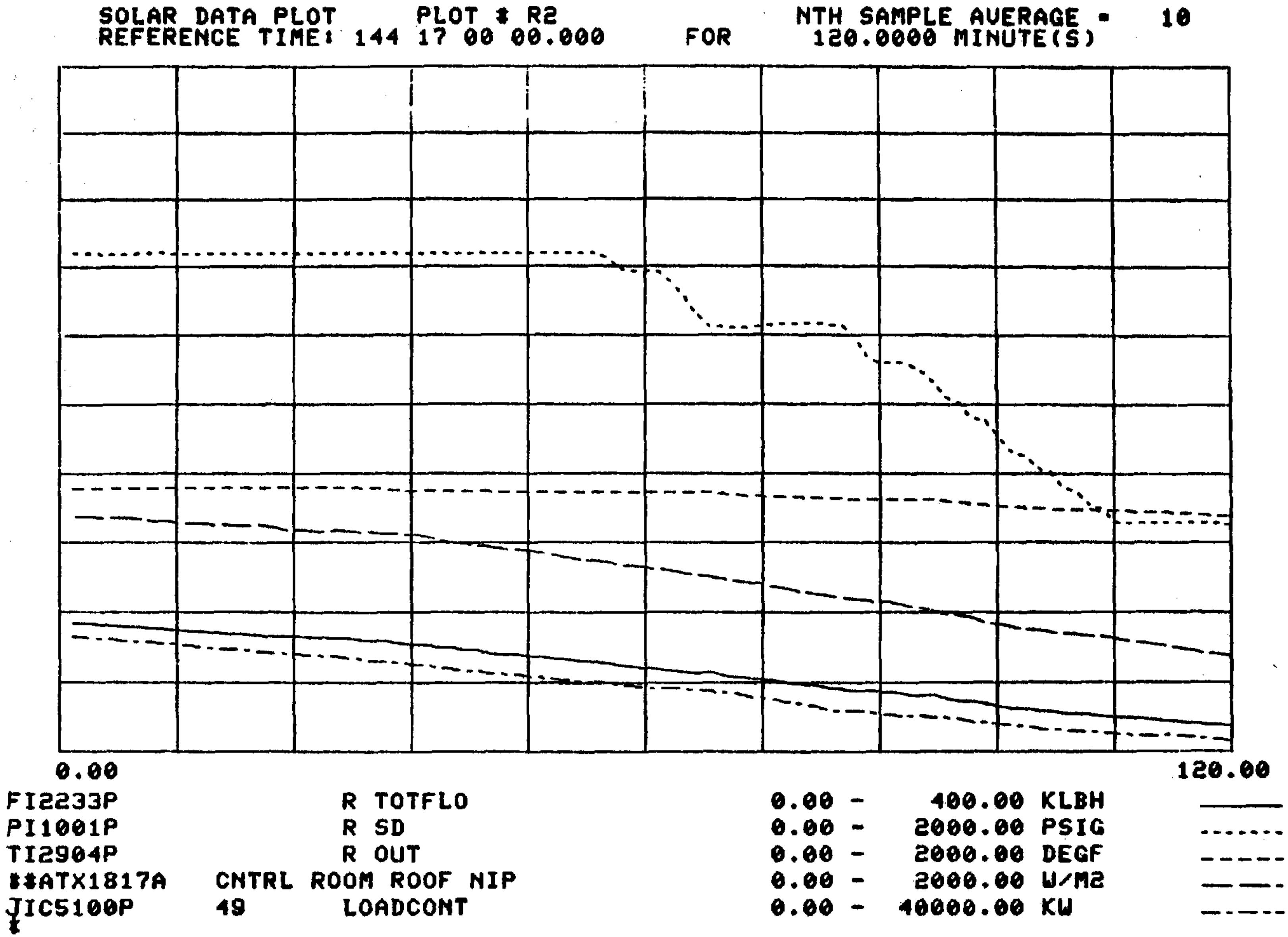

Figure 5.14. Major Mode 1 Plant Parameters, Day 144 (5/24/83) 17:00 – 19:00 Hrs

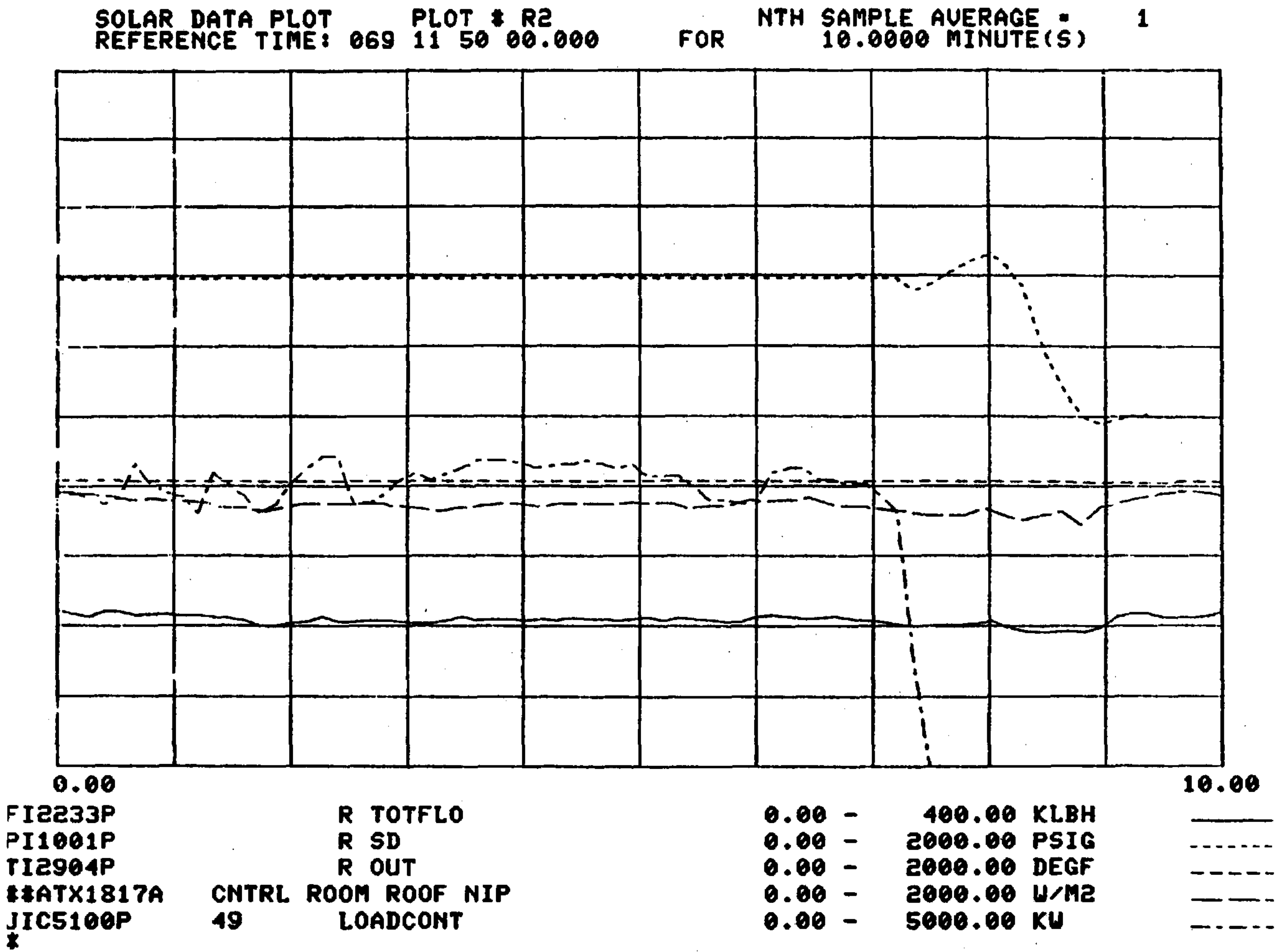

Figure 5.15. System Behavior in Response to Turbine Trip

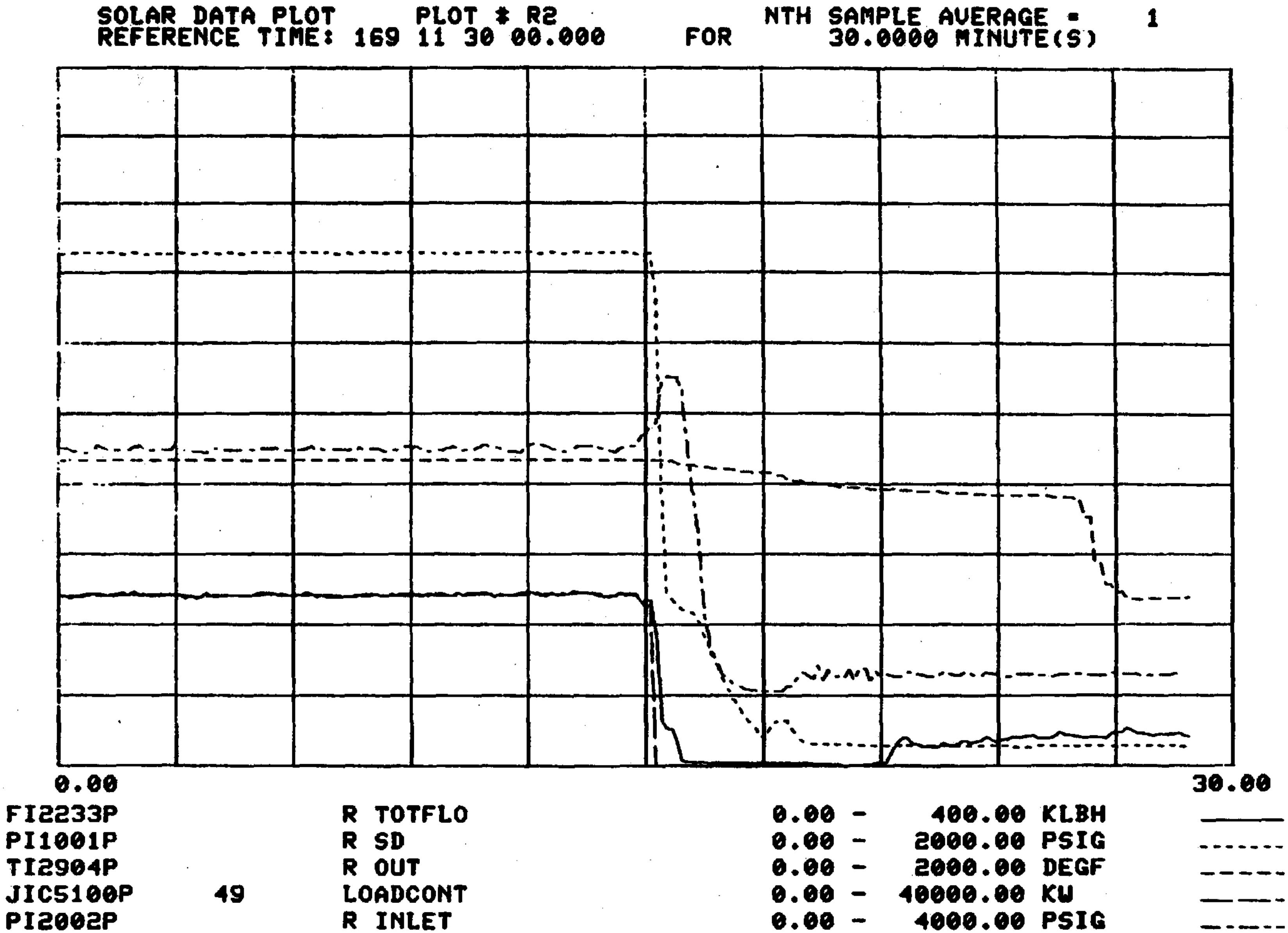

Figure 5.16. System Behavior in Response to Receiver Trip

following the trip. The feedwater pressure (PI2002) was subsequently reduced through a simple set point reduction. The steam temperature trace (TI2904) shows that the receiver discharge temperature remained near its operating level for a substantial period until feedwater circulation was reestablished through the receiver.

During both of these trip events, the trip logic and related process-control provisions responded in a manner consistent with the design intent. In both cases, the trips shut down that portion of the plant experiencing the problem and maintained the plant in a safe condition.

6.0 Conclusions

The Mode 1 testing has accomplished most of the explicit and implicit test objectives associated with this mode of plant operation. The exceptions are in the area of maintaining at least 10 MW of net power production for 4 and 7.8 hours respectively to simulate "design" winter and summer day operation. The principal reasons that these objectives have not been demonstrated involve continuing low insolation levels, heliostat cleanliness, and heliostat availability relative to their respective design values. As plant and insolation conditions permit, continuing Mode 1 "duration" testing should be carried out to demonstrate this objective.

From a steady state standpoint, the test results indicate that a performance improvement can be realized by operating the plant at reduced steam temperature and pressure relative to the design point operating conditions of 960°F and 1450 psi. These performance improvements associated with off design operating conditions are due to: (1) the turbine's relative performance insensitivity to steam temperature; (2) improved turbine expansion efficiency and reduced control valve losses associated with higher flow, reduced pressure operation; (3) reduced receiver heat losses resulting from lower receiver operating temperature; and (4) lower parasitic power demands associated with lower pressure operation.

Modifications to the basic Mode 1 operating procedures have been made based on these conclusions. During the high power midday period, steam conditions of 850°F and 1300 psi are selected which result in the turbine main steam control valve operating at 80 - 85% open. As the normal afternoon reduction in available power occurs, gradual reductions in steam temperature to 650 - 700°F and steam pressure to 700 - 750 psi are made subject to the constraint of maintaining at least 100°F of superheat at all times.

From the standpoint of Mode 1 transitions, the testing demonstrated that the turbine generator could be reasonably brought on line within 2 - 2-1/2 hours following sunrise while the same sequence could be executed in 1 1-1/2 hours for a midday start. The testing also showed that operation can continue down to power levels of approximately 0.5 MW through controlled reduction in steam conditions. This operation typically approaches to within 45 minutes of sunset during a clear day.

Trip sequences involving the turbine and receiver demonstrated that the trip logic and controlled sequences were properly executed to protect plant equipment and to maintain safe plant operation.

List of References

1. Pilot Plant Station Manual (RADL Item 2-1), Volume 1, System Description. Revised September 1982. Prepared by McDonnell Douglas Astronautics Company under Department of Energy Contract DE-AC03-79SF10499.

2. Same as Reference 1. Note: Some of the current waterfall parameters have been revised relative to those shown in Reference 1 to reflect final equipment (supplier provided) data regarding turbine performance and heliostat reflective area.

3. Collector Field Optimization Report (RADL Item 2-25). Revised January 1981. Prepared by the McDonnell Douglas Astronautics Company under Department of Energy Contract DE-AC03-79SF10499.

4. Solar One Generating Station Operation Manual, GEK-71561. Turbine No. 197845. Prepared by General Electric for Southern California Edison.

5. Heat and Mass Balance Design Analysis (RADL Item 2-15). Revised February 1980. Prepared by McDonnell Douglas Astronautics Company under Department of Energy Contract DE-AC03-79SF10499.

6. Central Receiver Solar Thermal Power System Phase I Pilot Plant Preliminary Design Report, Vol IV, Receiver Subsystem, SAN-1108-76-8. Prepared by the McDonnell Douglas Astronautics Company, October 1977.

7. PSS Final Design Calculations, Book 26 of 26--MDAC General Analysis and Background Data (RADL Item 7-8), September 1980. Prepared by the McDonnell Douglas Astronautics Company under Department of Energy Contract DE-AC03-79SF10499.

NOTE OF EXPLANATION

Day numbering schemes:

Generally, day numbers reported here are sequential beginning with 1 January being day 1. One exception, based upon the source calculation is made; Blocking and Shadowing, and Cosine Tables 3.1 and 3.2 are based upon day 1 being Spring equinox. Sun position is symmetrical about that date, March 20, calendar day number 79. To obtain the Julian day number on Tables 3.1 and 3.2, subtract 79 if the date is before March 20, and add if after March 20.

UNLIMITED RELEASE
INITIAL DISTRIBUTION

U.S. Department of Energy (4)
Forrestal Building, Room 5H021
Code CE-314
1000 Independence Avenue, S.W.
Washington, D.C. 20585
Attn: C. Carwile
H. Coleman
F. Morse
M. Scheve

U. S. Department of Energy (2)
P.O. Box 5400
Albuquerque, NM 87115
Attn: D. Graves
J. Weisiger

U.S. Department of Energy
Solar One Field Office
P.O. Box 366
Daggett, CA 92327

U.S. Department of Energy (4)
1333 Broadway
Oakland, CA 94612
Attn: T. Heenan
R. Hughey
G. Katz
W. Lambert

University of California
Environmental Science and Engineering
Los Angeles, CA 90024
Attn: R. G. Lindberg

University of Houston
Solar Energy Laboratory
4800 Calhoun
Houston, TX 77704
Attn: A. F. Hildebrandt

AMFAC
P.O. Box 3230
Honolulu, HI 96801
Attn: G. E. St. John

ARCO Power Systems
7061 S. University, Suite 300
Littleton, CO 80122
Attn: F. A. Blake

ARCO Power Systems
302 Nichols Drive
Hutchins, TX 75141
Attn: R. L. Henry

Arizona Public Service Company
P.O. Box 21666
Phoenix, AZ 85036
Attn: E. Weber

Babcock and Wilcox (3)
91 Stirling Avenue
Barberton, OH 44203
Attn: G. Grant
M. Seale
D. C. Smith

Bechtel Group, Inc.
P.O. Box 3965
San Francisco, CA 94119
Attn: G. W. Braun

Black & Veatch Consulting Engineers (2)
P.O. Box 8405
Kansas City, MO 64114
Attn: J. C. Grosskreutz
S. L. Levy

Boeing Engineering and Construction Company
P.O. Box 3707
Seattle, WA 98124
Attn: R. L. Campbell

California Energy Commission
1516 Ninth St., M/S 40
Sacramento, CA 95814
Attn: A. Jenkins

Combustion Engineering, Inc.
1000 Prospect Hill Road
Winsor, CT 06095
Attn: C. R. Buzzuto

El Paso Electric Company
P.O. Box 982
El Paso, TX 79946
Attn: J. E. Brown

Electric Power Research Institute (2)
P.O. Box 10412
Palo Alto, CA 94303
Attn: J. Bigger
E. DeMeo

Exxon Enterprises, Inc.
P.O. Box 592
Florham Park, NJ 07932
Attn: T. L. Guckes

Foster Wheeler Development Co.
12 Peach Tree Hill Road
Livingston, NJ 07039
Attn: R. J. Zoschak

Georgia Institute of Technology
Atlanta, GA 30332
Attn: C. T. Brown

Jet Propulsion Laboratory
4800 Oak Grove Drive
Pasadena, CA 91103
Attn: M. Alper

Los Angeles Department of Water and Power
Alternate Energy Systems
P.O. Box 111
111 North Hope St.
Los Angeles, CA 90051
Attn: D. Chu

Meridian Corporation
5113 Leesburg Pike
Falls Church, VA 22041
Attn: R. King

Martin Marietta Aerospace
P.O. Box 179, MS L0450
Denver, CO 80201
Attn: H. Wroton

McDonnell Douglas Astronautics Company
5301 Bolsa Avenue
Huntington Beach, CA 92647
Attn: R. L. Gervais
H. H. Dixon
J. E. Raetz (10)

Olin Chemicals Group
120 Long Ridge Road
Stamford, CT 06904
Attn: F. N. Christopher
L. C. Fiorucci

Pacific Gas and Electric Company
77 Beale Street
San Francisco, CA 94105
Attn: R. Molano
R. E. Price

Pacific Gas and Electric Company
3400 Crow Canyon Road
San Ramon, CA 94526
Attn: C. Weinberg

Pioneer Mill Company (AMFAC)
P.O. Box 727
Lahaina, HI 96761
Attn: R. K. MacMillan

Rockwell International
Energy Systems Group
8900 De Soto Avenue
Canoga Park, CA 91304
Attn: T. Springer

Rockwell International
Rocketdyne Division
6633 Canoga Avenue
Canoga Park, CA 91304
Attn: J. Friefeld

Solar Energy Industries Association
1140 19th St. N.W.
Suite 600
Washington, D.C. 20036
Attn: C. LaPorta

Solar Energy Research Institute (2)
1617 Cole Boulevard
Golden, CO 80401
Attn: B. Gupta
R. Hulstram

Southern California Edison
P.O. Box 325
Daggett, CA 92327
Attn: C. Lopez
P. Tong-Snyder (50)

Southern California Edison
P.O. Box 800
Rosemead, CA 92807
Attn: J. N. Reeves
P. Skvarna (25)

Stearns-Roger
P.O. Box 5888
Denver, CO 80217
Attn: W. R. Lang

Stone and Webster Engineering Corporation
P.O. Box 1214
Boston, MA 02107
Attn: R. W. Kuhr

Westinghouse Electric Corporation
Advanced Energy Systems Division
P.O. Box 10864
Pittsbugh, PA 15236
Attn: J. R. Maxwell

E. H. Beckner, 6000; Attn: V. Dugan, 6200
D. G. Schueler, 6220
J. V. Otts, 6222
R. S. Claassen, 8000; Attn: D. M. Olson, 8100
A. N. Blackwell, 8200
D. L. Hartley, 8300
C. S. Selvage, 8000A
C. Hartwig, 8244
M. E. John, 8245
R. C. Wayne, 8400; Attn: L. D. Bertholf, 8430
H. Hanser, 8440
R. L. Rinne, 8470
J. B. Wright, 8450
A. C. Skinrood, 8452 (25)
D. N. Tanner, 8452
J. C. Swearengen, 8453
J. B. Wright, 8454 (Actg.)

Publications Division 8265, for TIC (27)
Publications Division 8265/Technical Library Processes Division, 3141
Technical Library Processes Division, 3141 (3)
M. A. Pound, 8024, for Central Technical Files (3)